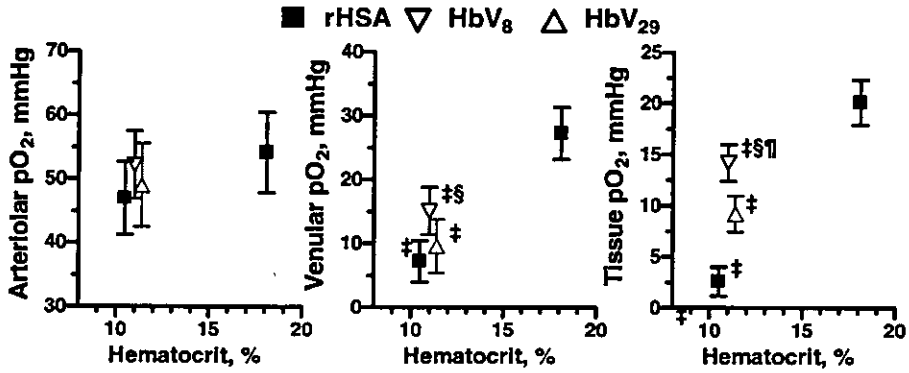

Fig. 7. Intravascular P_{O_2} after the *level 2* and *level 3* hemodilutions. Values are presented as means ± SD. ‡$P < 0.05$ compared with *level 2* with rHSA; §$P < 0.05$ compared with *level 3* with rHSA; ¶$P < 0.05$, *level 3* with HbV_8 vs. *level 3* with HbV_{29}.

where the anoxic threshold is passed, thus eliminating the inherent variability of oxygen delivery shown by the variability of tissue P_{O_2}.

Considering the significantly improved blood pressure and the trend toward higher flow for HbV_8 (in the absence of vasoconstriction and changes in the rheological properties of blood), it is possible that in conditions of extreme hemodilution the cardiac function should be improved because of the proposed more homogenous heart tissue oxygenation using HbV_8 vs. HbV_{29}.

In summary, the present results show that either HbV_8 or HbV_{29} are efficient oxygen carriers that do not cause vasoactivity. The experiments were carried out using rHSA as a hemodiluent, and this material was adequate as a plasma volume substitute. Oxygen extraction was similar for both oxygen carriers; however, HbV_8 appeared to be beneficial at the systemic level, because base excess remained at baseline levels, whereas it was decreased for HbV_{29}. This finding suggests that improved tissue P_{O_2} and microcirculatory oxygen delivery may be efficient in other tissues. The improvement obtained may be specific to the conditions of these experiments in which the vesicles were tested for their capacity to restore tissue P_{O_2}, FCD, and oxygen extraction in the microcirculation during extreme hemodilution. The significant differences in the tissue oxygen parameters produced by the presence of low-P_{50} Hbs vs. an identical oxygen carrier with normal P_{50} suggests that small amounts of Hbs with high oxygen affinity may have therapeutic effects in the treatment of ischemic conditions (6).

ACKNOWLEDGMENTS

We greatly acknowledge A. Barra and C. Walter (Univ. of California-San Diego) for technical assistance and Drs. K. Sou and Y. Teramura (Waseda University) for preparation of the HbV suspension.

GRANTS

This work was supported by National Heart, Lung, and Blood Institute (NHLBI) Bioengineering Research Partnership Grant R24-HL-64395, NHLBI Grants R01-HL-62354 and R01-HL-62318 (to M. Intaglietta), and NHLBI Program Project Grant P01-HL-71064-01 (to Dr. J. Friedman) and by U.S. Army Grant PR023085, Health Sciences Research Grants (Research on Regulatory Science), the Ministry of Health, Labour, and Welfare, Japan, and grants in aid for Scientific Research from the Japan Society for the Promotion of Science (B16300162).

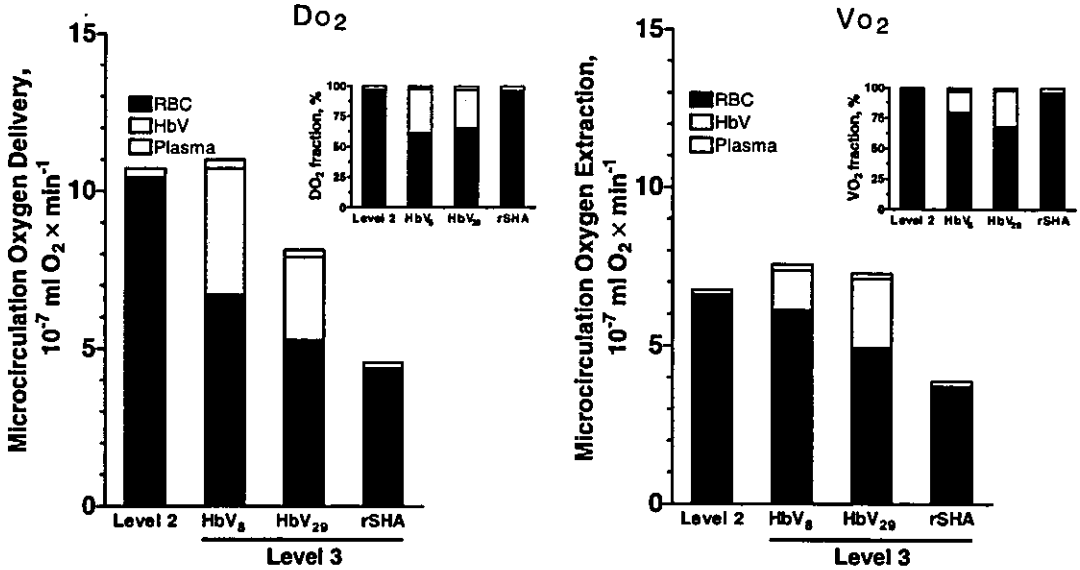

Fig. 8. Arterial oxygen delivery (D_{O_2}) and extraction (V_{O_2}) before and after the *level 3* hemodilution. Calculations of global oxygen transport are not directly measurable in our model; however, the changes relative to baseline can be calculated using the measured parameters. These calculations can be identified as those presented without standard deviations to focus on their tendencies rather than on the variability of the measurement.

REFERENCES

1. **Altman DG and Bland JM.** Statistics notes: how to randomise. *BMJ* 319: 703–704, 1999.
2. **Baines AD and Drangova R.** Does dopamine use several signal pathways to inhibit Na-Pi transport in OK cells? *J Am Soc Nephrol* 9: 1604–1612, 1998.
3. **Baines AD and Ho P.** O_2 affinity of cross-linked hemoglobins modifies O_2 metabolism in proximal tubules. *J Appl Physiol* 95: 563–570, 2003.
4. **Cabrales P, Kanika ND, Manjula BN, Tsai AG, Acharya SA, and Intaglietta M.** Microvascular Po_2 during extreme hemodilution with hemoglobin site specifically PEGylated at Cys-93(β) in hamster window chamber. *Am J Physiol Heart Circ Physiol* 287: H1609–H1617, 2004.
5. **Cabrales P, Tsai AG, and Intaglietta M.** Microvascular pressure and functional capillary density in extreme hemodilution with low and high plasma viscosity expanders. *Am J Physiol Heart Circ Physiol* 287: H363–H373, 2004.
6. **Endrich B, Asaishi K, Götz A, and Messmer K.** Technical report: a new chamber technique for microvascular studies in unanaesthetized hamsters. *Res Exp Med (Berl)* 177: 125–134, 1980.
7. **Hogan MC, Bebout DE, and Wagner PD.** Effect of increased Hb-O_2 affinity on $Vo_{2\,max}$ at constant O_2 delivery in dog muscle in situ. *J Appl Physiol* 70: 2656–2662, 1991.
8. **Intaglietta M, Silverman NR, and Tompkins WR.** Capillary flow velocity measurements in vivo and in situ by television methods. *Microvasc Res* 10: 165–179, 1975.
9. **Kerger H, Groth G, Kalenka A, Vajkoczy P, Tsai AG, and Intaglietta M.** pO_2 measurements by phosphorescence quenching: characteristics and applications of an automated system. *Microvasc Res* 65: 32–38, 2003.
10. **Lipowsky HH and Firrell JC.** Microvascular hemodynamics during systemic hemodilution and hemoconcentration. *Am J Physiol Heart Circ Physiol* 250: H908–H922, 1986.
11. **Lipowsky HH and Zweifach BW.** Application of the "two-slit" photometric technique to the measurement of microvascular volumetric flow rates. *Microvasc Res* 15: 93–101, 1978.
12. **Sakai H, Hara H, Yuasa M, Tsai AG, Takeoka S, Tsuchida E, and Intaglietta M.** Molecular dimensions of Hb-based O_2 carriers determine constriction of resistance arteries and hypertension. *Am J Physiol Heart Circ Physiol* 279: H908–H915, 2000.
13. **Sakai H, Masada Y, Horinouchi H, Yamamoto M, Ikeda E, Takeoka S, Kobayashi K, and Tsuchida E.** Hemoglobin-vesicles suspended in recombinant human serum albumin for resuscitation from hemorrhagic shock in anesthetized rats. *Crit Care Med* 32: 539–545, 2004.
14. **Sakai H, Tomiyama KI, Sou K, Takeoka S, and Tsuchida E.** Polyethyleneglycol-conjugation and deoxygenation enable long-term preservation of hemoglobin-vesicles as oxygen carriers in a liquid state. *Bioconjug Chem* 11: 425–432, 2000.
15. **Sakai H, Tsai AG, Intaglietta M, and Tsuchida E.** Hemoglobin encapsulation with polyethylene glycol-modified and unmodified vesicles: systemic and microvascular hemodynamics at 80% blood substitution. In: *Advances in Blood Substitutes. Industrial Opportunities and Medical Challenges*, edited by Winslow RM, Vandegriff KD, and Intaglietta M. Boston, MA: Birkhäuser, 1997, p. 151–166.
16. **Sakai H, Tsai AG, Rohlfs RJ, Hara H, Takeoka S, Tsuchida E, and Intaglietta M.** Microvascular responses to hemodilution with Hb vesicles as RBC substitutes: influence of O_2 affinity. *Am J Physiol Heart Circ Physiol* 276: H553–H562, 1999.
17. **Sou K, Endo T, Takeoka S, and Tsuchida E.** Poly(ethylene glycol)-modification of the phospholipid vesicles by using the spontaneous incorporation of poly(ethylene glycol)-lipid into the vesicles. *Bioconjug Chem* 11: 372–379, 2000.
18. **Torres Filho IP and Intaglietta M.** Microvessel Po_2 measurements by phosphorescence decay method. *Am J Physiol Heart Circ Physiol* 265: H1434–H1438, 1993.
19. **Tsai AG.** Influence of cell-free hemoglobin on local tissue perfusion and oxygenation after acute anemia after isovolemic hemodilution. *Transfusion* 41: 1290–1298, 2001.
20. **Tsai AG, Friesenecker B, Mazzoni MC, Kerger H, Buerk DG, Johnson PC, and Intaglietta M.** Microvascular and tissue oxygen gradients in the rat mesentery. *Proc Natl Acad Sci USA* 95: 6590–6595, 1998.
21. **Tsai AG, Friesenecker B, McCarthy M, Sakai H, and Intaglietta M.** Plasma viscosity regulates capillary perfusion during extreme hemodilution in hamster skin fold model. *Am J Physiol Heart Circ Physiol* 275: H2170–H2180, 1998.
22. **Tsai AG, Vandegriff KD, Intaglietta M, and Winslow RM.** Targeted O_2 delivery by low-P_{50} hemoglobin: a new basis for O_2 therapeutics. *Am J Physiol Heart Circ Physiol* 285: H1411–H1419, 2003.
23. **Webb AR, Barclay SA, and Bennett ED.** In vitro colloid osmotic pressure of commonly used plasma expanders and substitutes: a study of the diffusibility of colloid molecules. *Intensive Care Med* 15: 116–120, 1989.

taprald4/zh4-ahea/zh4-ahea/zh400605/zh43937d05g | sweigarl | S=5 | 3/16/05 | 16:20 | MS: H1184-4 | Ini: 06e/kmp\bew | input-dms

Am J Physiol Heart Circ Physiol 288: H000–H000, 2005.
First published January 28, 2005; doi:10.1152/ajpheart.01184.2004.

Oxygen release from low and normal P_{50} Hb vesicles in transiently occluded arterioles of the hamster window model

Hiromi Sakai,[1] Pedro Cabrales,[2,3] Amy G. Tsai,[2,3] Eishun Tsuchida,[1] and Marcos Intaglietta[2,3]

[1]*Advanced Research Institute for Science and Engineering, Waseda University, Tokyo, Japan; and* [2]*Department of Bioengineering, University of California-San Diego, and* [3]*La Jolla Bioengineering Institute, La Jolla, California*

Submitted 27 November 2004; accepted in final form 24 January 2005

Sakai, Hiromi, Pedro Cabrales, Amy G. Tsai, Eishun Tsuchida, and Marcos Intaglietta. Oxygen release from low and normal P_{50} Hb vesicles in transiently occluded arterioles of the hamster window model. *Am J Physiol Heart Circ Physiol* 288: H000–H000, 2005. First published January 28, 2005; doi:10.1152/ajpheart.01184.2004.—A phospholipid vesicle encapsulating Hb [Hb vesicle (HbV)] has been developed as a transfusion alternative. One characteristic of HbV is that the O_2 affinity [P_{O_2} at which Hb is 50% saturated (P_{50})] of Hb can be easily regulated by the amount of the coencapsulated allosteric effector pyridoxal 5′-phosphate. In this study, we prepared two HbVs with different P_{50}s (8 and 29 mmHg, termed HbV_8 and HbV_{29}, respectively) and observed their O_2-releasing behavior from an occluded arteriole in a hamster skinfold window model. Conscious hamsters received HbV_8 or HbV_{29} at a dose rate of 7 ml/kg. In the microscopic view, an arteriole (diameter: 53.0 ± 6.6 μm) was occluded transcutaneously by a glass pipette on a manipulator, and the reduction of the intra-arteriolar P_{O_2} 100 μm down from the occlusion was measured by the phosphorescence quenching of preinfused Pd-porphyrin. The baseline arteriolar P_{O_2} (50–52 mmHg) decreased to about 5 mmHg for all the groups. Occlusion after HbV_8 infusion showed a slightly slower rate of P_{O_2} reduction compared with that after HbV_{29} infusion. The arteriolar O_2 content was calculated at each reducing P_{O_2} in combination with the O_2 equilibrium curves of HbVs, and it was clarified that HbV_8 showed a significantly slower rate of O_2 release compared with HbV_{29} and was a primary source of O_2 (maximum fraction, 0.55) overwhelming red blood cells when the P_{O_2} was reduced (e.g., <10 mmHg) despite a small dosage of HbV. This result supports the possible utilization of Hb-based O_2 carriers with lower P_{50} for oxygenation of ischemic tissues.

blood substitutes; artificial red blood cells; occlusion; microhemodynamics; liposome

PHOSPHOLIPID VESICLES encapsulating concentrated human Hb [Hb vesicles (HbV)] or liposome-encapsulated Hb can serve as a transfusion alternative whose O_2 carrying capacity can be formulated to be comparable to that of blood (1, 5, 8, 16, 24, 30). The capsular structure of HbV (particle diameter ~250 nm) has characteristics similar to those of natural red blood cells (RBCs), because both have membranes that prevent direct contact of Hb with the components of blood and the endothelial lining, mitigating cellular injury due to Hb-mediated prooxidative species (4, 38). Furthermore, Hb encapsulation in vesicles prevents a hypertensive response induced by free Hbs that scavenge the endogenous vasorelaxation factors nitric oxide (NO) and carbon monoxide (12, 18, 26). The safety of HbV has been confirmed in rodent models in terms of the prompt metabolism of the components of HbV in the reticuloendothelial system, which was demonstrated by histopathological analysis and plasma biochemical analysis (28, 29).

One of the characteristics of the capsular HbV is that its physicochemical characteristics such as O_2 affinity [O_2 tension at which Hb is half-saturated with O_2 (P_{50})] can be easily regulated by manipulating the amount of an allosteric effector coencapsulated in HbV. This property provides additional flexibility in formulating the O_2 transport properties of HbV by comparison with the chemically modified Hbs whose P_{50} is modified and fixed by chemical reactions such as cross-linking or polymer conjugation (34). We use pyridoxal 5′-phosphate (PLP) as the allosteric effector (33, 45). For example, coencapsulation of PLP at the molar ratio of PLP to Hb of 2.5:1 yields a P_{50} of about 29 mmHg. On the other hand, HbVs without PLP have a P_{50} of 8 mmHg. Historically, P_{50} was set similar to that of RBCs or about 25–30 mmHg, which theoretically allows sufficient O_2 unloading as blood transits the microcirculation. Decreasing O_2 affinity (increasing P_{50}) increases O_2 unloading in the peripheral blood circulation as shown by the enhanced O_2 release and improved exercise capacity in mutant mice that carry high P_{50} RBCs (36).

Hemoglobin-based O_2 carriers (HBOCs) of molecular dimensions as well as HbV could be effective for the targeted oxygenation of ischemic tissues (6, 43) because the small particle dimension would allow their passage through constricted or partially occluded vessels that do not allow the passage of RBCs (19). Blood flow in these vessels and in collateral vessels is usually slow, thus increasing RBC transit times (7, 11). As a result, tissue P_{O_2} is low and RBCs release most of their O_2 before reaching the capillary circulation. As an example, if tissue P_{O_2} is below 5 mmHg, O_2 saturation (Sa_{O_2}) of RBCs would be around 5%, and RBCs will have released most of their O_2 before they reach the ischemic tissue. Thus an HBOC with a normal P_{50} similar to RBCs would not be effective for carrying O_2 to the ischemic tissue.

In this study, we evaluate the rate of O_2 release from HbVs with high and low P_{50}s from arterioles immediately after their occlusion. We selected arterioles with diameters of about 50 μm because this size of arterioles contributes significantly to tissue oxygenation in normal conditions (13). This model was selected to determine the ability of HbVs to retain or release O_2 in hypoxic conditions and establish their suitability for oxygenating ischemic tissues.

Address for reprint requests and other correspondence: E. Tsuchida, Advanced Research Institute for Science and Engineering, Waseda Univ., Tokyo 169-8555, Japan (E-mail: eishun@waseda.jp).

The costs of publication of this article were defrayed in part by the payment of page charges. The article must therefore be hereby marked "*advertisement*" in accordance with 18 U.S.C. Section 1734 solely to indicate this fact.

MATERIALS AND METHODS

Preparation of HbVs. HbVs with different P_{50}s were prepared under sterile conditions as previously reported (32, 34, 37). Hb was purified from outdated donated human blood provided by the Japanese Red Cross Society (Tokyo, Japan). HbVs with a P_{50} = 29 mmHg (HbV_{29}) was prepared by adding the allosteric effector pyridoxal 5′-phosphate (PLP; 14.7 mM, Sigma Chemical; St. Louis, MO) to Hb (38 g/dl) at a molar ratio of PLP to Hb = 2.5. HbVs with a P_{50} = 8 mmHg (HbV_8) were prepared by adding no allosteric effector to the Hb solution. The Hb solution was encapsulated within vesicles composed of Presome PPG-I [a mixture of 1,2-dipalmitoyl-*sn*-glycero-3-phosphatidylcholine, cholesterol, and 1,5-di-*O*-octadecyl-*N*-succinyl-L-glutamate at a molar ratio of 5:5:1 (Nippon Fine Chemicals; Osaka, Japan)], and the particle size of HbVs was regulated by an extrusion method. The surface of the HbVs was modified with polyethylene glycol (molecular mass: 5 kDa, 0.3 mol% of the lipids in the outer surface of vesicles) using 1,2-distearoyl-*sn*-glycero-3-phosphatidylethanolamine-*N*-polyethylene glycol (Sunbright DSPE-50H, H-form, NOF; Tokyo, Japan). HbVs were suspended in a physiological salt solution and sterilized with filters (Dismic, Toyo Roshi; Tokyo, Japan; pore size: 0.45 μm) and deoxygenated with N_2 bubbling for storage. The endotoxin content was measured with a modified LAL assay, and the level was less than 0.2 EU/ml (27). The O_2 equilibrium curves (OECs) of HbV_{29} and HbV_8 were obtained by a Hemox Analyzer (TCS-Medical Products; Philadelphia, PA), as shown in Fig. 1. The physicochemical parameters of the HbVs are listed in Table 1.

Animal model and preparation. Experiments were carried out in 12 male Syrian golden hamsters (59 ± 12 g body wt, Charles Rivers; Worcester, MA). The dorsal skinfold consisting of two layers of skin and muscle was fitted with two titanium frames with a 15-mm circular opening and surgically installed under intraperitoneal pentobarbital sodium anesthesia (~50 mg/kg body wt, Abbott Laboratory; North Chicago, IL). After the hair on the back skin of the hamster was removed, layers of skin muscle were separated from the subcutaneous tissue and removed until a thin monolayer of muscle including the small artery and vein and one layer of intact skin remained. A coverglass (diameter 12 mm) held by one frame covered the exposed tissue allowing intravital observation of the microcirculation (20, 22, 25).

Polyethylene (PE) tubes (PE-10, Becton-Dickinson; Parsippany, NJ; ~1 cm) were connected to PE-50 tubing (~25 cm) via silicone elastomer medical tubes (~4 cm, Technical Products; Decatur, GA) and were implanted in the jugular vein and the carotid artery. They were passed from the ventral to the dorsal side of the neck and exteriorized through the skin at the base of the chamber. Patency of the catheters was ensured by filling them with heparinized saline (40 IU/ml). Microvascular observations of the awake and unanesthetized hamsters were performed 5 days after chamber implantation to mitigate the effects of surgery. The hamster was placed in a perforated plastic tube from which the window chamber protruded to minimize animal movement without impeding respiration. All animal studies were approved by the Animal Care and Use Committee of University of California-San Diego and performed according to the National Institutes of Health *Guide for the Care and Use of Laboratory Animals* (Washington, DC: National Academy Press, 1996).

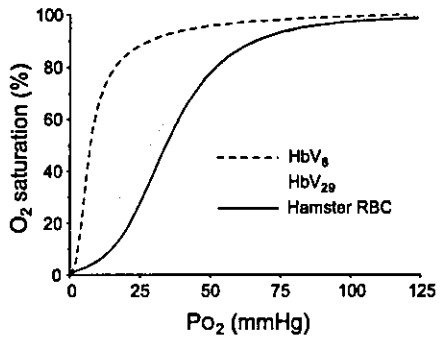

Fig. 1. Oxygen equilibrium curves (OECs) of Hb vesicles (HbVs) at a Po_2 where Hb is half-saturated (P_{50}) of 8 mmHg (HbV_8) and 29 mmHg (HbV_{29}) measured with a Hemox Analyzer (TCS Medical Products) at 37°C compared with hamster blood. RBC, red blood cells.

Table 1. *Physicochemical properties of HbV_8 and HbV_{29} compared with hamster blood*

Parameters	HbV_8	HbV_{29}	Hamster Blood
Hb concentration, g/dl	10	10	14.8 ± 0.5
Particle diameter, nm	250 ± 64	247 ± 44	5,000–7,000*
P_{50}, mmHg	8	29	28
Molar ratio of PLP to Hb	0	2.5	
MetHb, %	<3	<1	
HbCO, %	<2	<2	

HbV_8 and HbV_{29}, Hb vesicles (HbVs) at 8- and 29-mm Hg Po_2 at which Hb is 50% saturated (P_{50}); PLP, pyridoxal 5′-phosphate. *Size of hamster red blood cells (RBCs) (39).

Infusion of HbV_8 and HbV_{29} and occlusion of an arteriole. The unanesthetized animal was placed in a perforated plastic tube and stabilized under the microscope. Animals were suitable for the experiments if systemic variables were within normal range, namely, heart rate >340 beats/min, mean arterial pressure >80 mmHg, systemic hematocrit >45%, and arterial Po_2 >50 mmHg, and microscopic examination of the tissue in the chamber did not reveal signs of edema or bleeding. Baseline measurements of microvascular parameters and Po_2 (see below) were performed before the infusion of HbV_8 or HbV_{29} suspended in physiological saline solution into the venous line at 7 ml/kg. Systemic blood volume was estimated as 70 ml/kg. In our previous reports of resuscitation from hemorrhagic shock or hemodilution, HbVs were suspended in an albumin solution to regulate colloid osmotic pressure (30, 33). However, in the present study, we did not use albumin to minimize the hypervolemic effect. For the same reason, the infusion amount was minimized to equal 10% blood volume (7 ml/kg).

After we stabilized the condition and measured the systemic parameters for 20 min, diameter and blood flow of the selected arterioles were measured. Large feeding arterioles or small arcading arterioles (diameter 53.0 ± 6.6 μm) were selected for observation. The arterioles were occluded by means of a glass micropipette whose end was drawn into a long fiber by a pipette puller (Fig. 2). The fiber was bent over a flame, and the knee of the bend was used to press on the intact skin of the preparation mounted in an inverted microscope that allowed observation of the opposite side, i.e., the intact microcirculation. Once an arteriole was selected for measurement, the microoccluder is moved to the skin side, between the intact skin and the optics of the substage illumination. The tip of the occluder was placed near the center of the optical field of view of the microscope, and the vessel was similarly placed using the stage micrometric position control. This arrangement allowed for direct microscopic observation of the occluded vessel and the stopped flow as shown in Fig. 2. The duration of occlusion was 30 s.

Measurement of microhemodynamic parameters. Microvessels were observed by transillumination with an inverted microscope (IMT-2, Olympus; Tokyo, Japan). Microscopic images were video recorded (Cohu 4815-2000; San Diego, CA) and transferred to a television videocassette recorder (Sony Trinitron PVM-1271Q monitor; Tokyo, Japan) and Panasonic AG-7355 video recorder (Tokyo, Japan). Arterioles were classified according to their position within the microvascular network according to the previously reported scheme (33). Microvascular diameter and RBC velocity before occlu-

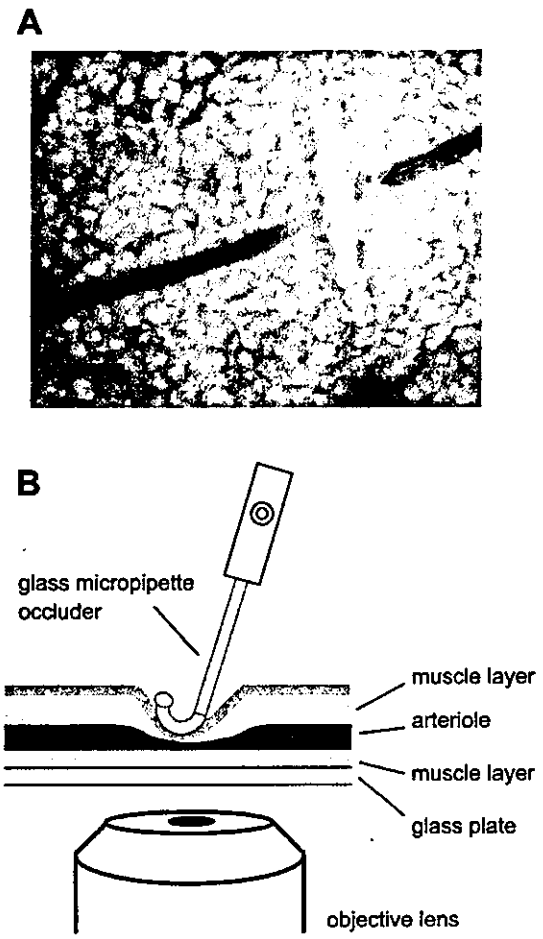

Fig. 2. *A*: microscopic image of an occluded arteriole in the hamster window chamber. The glass fiber lies across the arteriole. Scale bar = 100 μm. *B*: schematic representation of occlusion of *A* showing the different tissue layers of the skin (not to scale).

sion were analyzed on-line in the arterioles (14, 15). Vessel diameter was measured with an image-shearing system (Digital Video Image Shearing Monitor 908, I.P.M.; San Diego, CA), whereas RBC velocity was analyzed by photodiodes and the cross-correlation technique (Velocity Tracker Mod-102 B, I.P.M.). The blood flow rate (Q) was calculated using the following equation:

$$Q = (\text{RBC velocity}/R_v) \times (\text{diameter}/2)^2 \quad (1)$$

where $R_v = 1.6$ and is the ratio of the centerline velocity to average blood velocity according to data from glass tubes (20).

Palladium-porphyrin bound to bovine albumin solution (7.6 wt%, 0.1 ml) was injected intravenously 20 min before the infusion of HbVs. Arteriolar blood P_{O_2} was noninvasively determined by measuring the rate of decay of phosphorescence emitted by the metalloporphyrin complex after pulsed light excitation, which is a function of the local O_2 concentration (17, 40, 44). The relationship between phosphorescence lifetime and P_{O_2} is given by the following Stern-Volmer equation:

$$\tau_o/\tau = 1 + k_q \times \tau_o \times P_{O_2} \quad (2)$$

where τ_o and τ are the phosphorescence lifetimes in the absence of molecular O_2 and at a given P_{O_2}, respectively, and k_q is the quenching constant, with both factors being pH and temperature dependent. Light was gathered from an optical window of 20 × 5 μm placed longitudinally along the blood vessels. Measurements in the blood compartment were made every second using a single flash.

The P_{O_2} decay curves induced by the occlusion were obtained before the infusion of HbVs and 20 min after the infusion of HbVs. The Sa_{O_2} of HbVs at every P_{O_2} were obtained from the OECs (Fig. 1), and the total O_2 content in blood (ml O_2 in 1 dl blood) can be estimated using the following equation:

$$O_2 \text{ content} = 23.6 \times \frac{[Sa_{O_2}(\text{RBC}) + 0.0667 \times Sa_{O_2}(\text{HbV})]}{100} + 2.42 \times \frac{P_{O_2}}{713} \quad (3)$$

In this calculation, we used 15 g/dl as the average Hb concentration in arterial blood (14.8 ± 0.5 g/dl, heme concentration 9.3 mM), which was measured with a handheld photometer (B-Hemoglobin Photometer, Hemocue). One hundred milliliters of blood contain 23.6 ml O_2 bound to Hb when Sa_{O_2} is 100% (volume of an ideal gas at 37°C) according to Boyle-Charle's gas law, $PV = nRT$, where P (in atm) is atmospheric pressure, V (in liters) is gas volume, n is mole number, R is the gas constant (0.082 atm·l·K^{-1}·mol^{-1}), and T is absolute temperature [23.6 (ml) = 9.3 × 10^{-4} (mol) × 0.082 × (273 + 37) × 1,000]. The physically dissolved O_2 content at 1 atm O_2 (713 mmHg after subtracting the vapor pressure of water = 47 mmHg) at 37°C was calculated to be 2.42 ml in 100 ml water. Sa_{O_2}(RBC) and Sa_{O_2}(HbV) are Sa_{O_2}s of RBCs and HbVs, respectively, at each arteriolar P_{O_2} during the experiments.

HbVs were suspended in physiological saline solution ([Hb] = 10 g/dl); therefore, their infusion lowered colloid osmotic pressure, causing the extravasation of plasma fluid. To account for this, we carried out our measurements 20 min after HbV infusion and assumed that this interval was sufficient for normalizing blood volume through the release of extra fluid to the interstitium, thus increasing plasma Hb concentration by 6.7%.

Data analysis. Data are given as means ± SD for the indicated number of animals. Data were analyzed using ANOVA followed by Fisher's protected least-significant difference test between groups according to the previous studies. Student's *t*-test was used for comparisons within each group. All statistics were calculated using GraphPad Prism 4.01 (Graph Pad Software; San Diego, CA). Changes were considered statistically significant if $P < 0.05$.

RESULTS

Hemodynamic properties of arterioles. The profiles of the selected arterioles, diameters, centerline RBC velocities, blood flow rates, and intra-arteriolar P_{O_2} values before and after infusion of HbVs are listed in Table 2. There was no significant T2 difference between the groups. The O_2 content in blood attributed to hamster RBCs and physically dissolved O_2 at the observed arteriolar P_{O_2} was estimated as 18.61 ± 1.23 ml O_2/dl blood according to *Eq. 3*. After the infusion of HbV_8 and HbV_{29}, the O_2 content increased to 20.30 ± 1.18 and 20.17 ± 1.54 ml O_2/dl blood, respectively, due to the O_2 bound to HbVs. The contributions of HbV_8 and HbV_{29} to whole O_2 content were 1.51 ± 0.01 and 1.25 ± 0.07 ml O_2/dl blood, respectively. The HbV_8 group showed higher O_2 content than the HbV_{29} group due to the higher $Sa_{O_2}(HbV_8)$, which was 95.9 ± 0.6% compared with the $Sa_{O_2}(HbV_{29})$ of 79.6 ± 4.7%.

Changes in P_{O_2} in arterioles after occlusion in the presence of HbVs. Arteriolar P_{O_2} before occlusion was about 50–52 mmHg in average for all groups and started to decrease significantly immediately after occlusion, as shown in Fig. 3. F3 In all groups, P_{O_2} fell to about 10 and 5 mmHg after 10- and

tapraid4/zh4-ahea/zh4-ahea/zh400605/zh43937d05g | sweigart | S=5 | 3/16/05 | 16:20 | MS: H1184-4 | Ini: 06e/kmp\bew | Input-dms

Table 2. *Profiles of arterioles for occlusion before and after infusion of HbVs*

Parameters	Before Infusion	After HbV Infusion	
		HbV_8	HbV_{29}
Arteriolar diameter, μm	53.0±6.6	56.2±6.8	55.8±6.9
Centerline flow velocity, mm/s	3.1±0.5	3.4±0.7	3.5±0.5
Blood flow rate, nl/s	6.8±1.6	8.7±3.1	8.5±2.1
Arteriolar P_{O_2}, mmHg	50.7±4.7	51.4±4.8	52.1±5.3
Sa_{O_2}(RBC), %	78.1±5.1	76.0±7.7	77.9±6.5
Sa_{O_2}(HbV), %		95.9±0.6†	79.6±4.7
O_2 content in whole blood, ml/O_2/dl/blood	18.61±1.23	20.30±1.18*	20.17±1.54*
O_2 content in HbV, ml/O_2/dl/ blood		1.51±0.01	1.25±0.07

Values are means ± SD. Arteriolar P_{O_2}, O_2 saturation (Sa_{O_2}) and O_2 contents were obtained during 6 s before occlusion. *$P < 0.05$ vs. before infusion; †$P < 0.05$ vs. RBCs and HbV_{29}.

30-s occlusion, respectively. When the P_{O_2} values were expressed as relative to the baseline values (before occlusion), infusion of HbV_8 tended to show a slower rate of reduction of P_{O_2} compared with the infusion of HbV_{29} and without infusion (Fig. 4). There was a significant difference between the HbV_8 infusion and before infusion groups only at 7 s ($P = 0.035$).

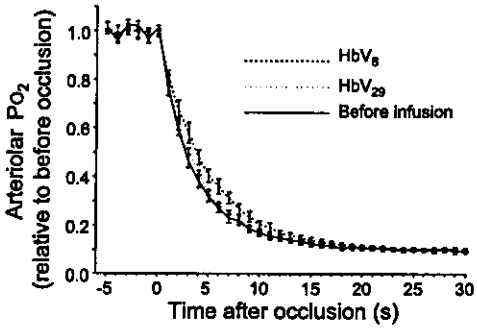

Fig. 4. Changes in P_{O_2} relative to before occlusion. The data in Fig. 3 were averaged. Baseline values before occlusion were obtained as the average of 6 values before occlusion and fixed as 1.0. There was a significant difference between the HbV_8 infusion and before infusion groups only at 7 s ($P = 0.035$).

Sa_{O_2}(RBC) and Sa_{O_2}(HbV) at every arteriolar P_{O_2} value can be estimated using the OECs in Fig. 1 assuming that the conditions in the arteriole (such as temperature and pH) do not change significantly from the normal condition (37°C, pH 7.4). Figure 5*A* shows the changes in the whole arteriolar O_2 content

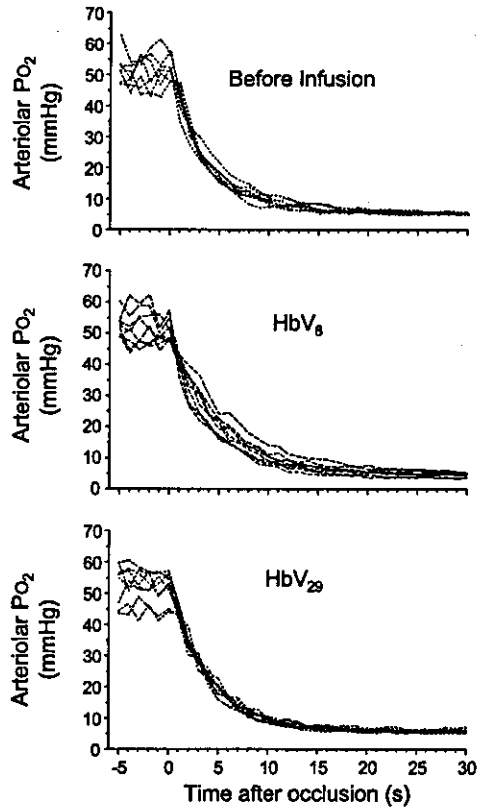

Fig. 3. Time course of P_{O_2} in the blood of an occluded arteriole (diameter, 53.0 ± 6.6 μm) before and after infusion of 7 ml/kg HbV_8 or HbV_{29} into hamsters. Measurements were made in blood at a distance of 50 μm from the point of occlusion. Most vessels equilibrate to intravascular partial pressure in the range of 4–6 mmHg about 15–20 s after occlusion.

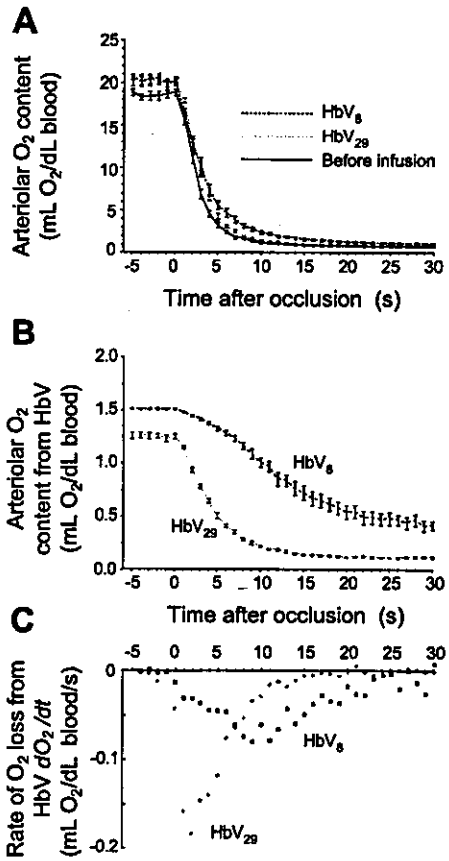

Fig. 5. *A*: time course of the arteriolar O_2 content in whole blood of an occluded arteriole before and after infusion of 7 ml/kg HbV_8 or HbV_{29} into hamsters. The O_2 contents were calculated using *Eq. 2* and the data of OECs (Fig. 1) and P_{O_2} changes (Fig. 3). *B*: time course of the O_2 content derived from HbVs in the blood. The contributions of HbVs are derived from the data in *A* and magnified in scale. *C*: rate of O_2 loss from HbVs. The graphs in *B* were differentiated and plotted.

during the occlusion. Immediately after occlusion, the O_2 content decreased rapidly. The HbV_8 group showed a slower rate of reduction compared with the HbV_{29} group and the group before HbV infusion. To demonstrate the contribution of HbVs clearly, only the O_2 content of HbVs is shown in Fig. 5*B*. HbV_8 showed a very slow rate of O_2 release. After 30 s of occlusion, the arteriolar P_{O_2} decreased to 5.2 ± 0.7 mmHg. However, $Sa_{O_2}(HbV_8)$ was 26.1 ± 7.3% and did not reach steady state but continued O_2 release. HbV_{29} showed almost no change after 15 s, and $Sa_{O_2}(HbV_{29})$ was 7.4 ± 1.0% after 30 s. Figure 5*C* shows the rate of O_2 loss from HbVs obtained by the differentiation of the graphs in Fig. 5B. HbV_{29} showed the fastest O_2 loss with the maximum of 0.18 ml O_2/dl blood sec after only 2 s of occlusion and did not supply O_2 after 17 s. On the other hand, HbV_8 showed a moderate O_2 loss and showed the maximum of 0.08 ml O_2/dl blood after 10 s of occlusion and continued to release O_2 until 30 s.

F6 Figure 6 shows the fraction of O_2 in blood originating from HbVs. Before occlusion of the arterioles, the fractions of HbV_8 and HbV_{29} are very small and similar because of the small dosage compared with the originally present RBCs. However, after occlusion, the fraction of O_2 from HbV_8 increased significantly and was about 0.55 after 10 s. This indicated that HbV_8, and not RBCs, was the main source of the O_2 carrier when P_{O_2} attained very low values.

DISCUSSION

The principal finding of this study is that HbV_8 (P_{50} = 8 mmHg) with a high O_2 affinity (low P_{50}) releases O_2 at a slower rate than does HbV_{29} in occluded arterioles of the hamster dorsal skinfold model. Furthermore, we found that HbV_8, and not HbV_{29}, is the main O_2 source in ischemic conditions.

The immediate occlusion of blood flow in the arterioles caused a rapid reduction of O_2 content. Similar phenomena have been observed by Richmond et al. (23) in rat spinotrapezius muscle tissue. There is substantial evidence that the arteriolar wall is a significant O_2 sink, consuming O_2 at a rate that is much greater than most tissues (9, 35, 42), which explains in part the significant and rapid drop of P_{O_2} found in our study. In our experiments, only one arteriole was occluded at a time in the intact subcutaneous tissue, and arteriolar P_{O_2} decreased to about 5 mmHg, which was higher than the critical P_{O_2} (2.9 ± 0.5 mmHg) in the rat spinotrapezius muscle tissue (23). Although the O_2 supply was significantly reduced, diffusion of O_2 from the other surrounding arterioles, venules, and capillaries near the occlusion should contribute to maintaining tissue P_{O_2} at a higher value than in the study of Richmond et al. (23), where the supply of blood to the tissue was stopped altogether. $Sa_{O_2}(HbV_8)$ at 5 mmHg is estimated to be about 26% according to the OECs (Fig. 1), which is higher than that for HbV_{29} (6%) and RBCs (2%); thus HbV_8 remains a source of O_2 for a longer period in a prolonged occlusion, because the fraction of O_2 from HbV_8 was 0.5 or higher, overwhelming the contribution from RBCs, as shown in Fig. 6.

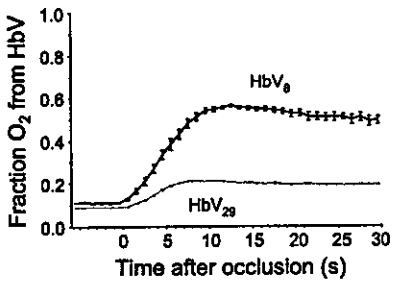

Fig. 6. Time course of the fraction of O_2 content from HbVs in whole blood. The extended time of occlusion induced hypoxic conditions and the fraction of O_2 content from HbV_8 increased significantly compared with HbV_{29}.

A limitation of our experimental method is that Sa_{O_2} is estimated under the assumption that conditions in the target arteriole are identical to that of the OEC measurement; however, the O_2 affinity of Hb changes as a function of temperature, pH, electrolyte concentration, and CO_2 content. Local ischemic conditions caused by the occlusion could affect pH and increase CO_2 tension, resulting in a slight decrease in the O_2 affinity (increased P_{50}); however, it is unlikely that this would introduce a significant error in the measurement of O_2 release considering the short duration of the occlusion (30 s).

We have previously demonstrated using an artificial narrow polymer tube (inner diameter: 28 μm) surrounded by a sodium dithionate solution to consume O_2 that a Hb solution under continuous flow conditions (1 mm/s) facilitates O_2 release when mixed with RBCs. Conversely, HbV did not show this phenomenon (31). This difference is due to the small size of O_2-bound acellular Hb molecules, which diffuse and therefore contribute to the facilitated O_2 transport (21, 31), whereas HbVs (diameter, about 250 nm) are too large to show sufficient diffusion for the facilitated O_2 transport. In these conditions, O_2 affinity (P_{50}) becomes the determining factor for the rate of O_2 release and transport to the vessels wall. Thus, in our present results, the presence of HbVs did not facilitate the reduction of P_{O_2} or O_2 content but retarded the reduction of P_{O_2} and O_2 content.

Our experimental model is designed to characterize the O_2 release behavior of blood from an occluded microvessel and does not directly related to clinical ischemic conditions because the occlusion of the small arteriole for 30 s does not induce tissue ischemia other than the transient event in the proximity of the microvessel. However, our data suggest that HbV_8 could be a significant source of O_2 in an ischemic condition with significantly lowered tissue P_{O_2}. Because of the small dosage of HbV_8 (10 ml/kg), the O_2 content in the blood after occlusion (5 ml O_2/dl blood at 5 s) is significantly smaller than the baseline value (20 ml O_2/dl blood at 0 s). To enhance the contribution of HbVs, a larger dosage and sustained blood flow would be required. Contaldo et al. (7) recently demonstrated that inducing hemodilution using up to 50% blood exchange with HbV (P_{50} = 15 mmHg) suspended in dextran effectively oxygenated ischemic collaterized tissue in skin flaps. This phenomenon could be explained by low P_{50} HbVs retaining O_2 in the upstream vessels and delivering it to the ischemic tissue via collateral arterioles, even when these may have significantly slower blood flow. It has been proposed that small-sized HBOCs oxygenate ischemic tissue by being able to pass through constricted or partially occluded vessels that do not allow the passage of RBCs; however, the results from Contaldo et al. (17) as well as those from our experimental model do not serve to support this concept, because arterioles were completely ligated or occluded. It should be noted, however, that an advantage of small HBOCs, including HbVs,

is that they are homogeneously dispersed in the plasma phase and therefore can deliver O_2 more homogeneously to the periphery than RBCs because microvascular hematocrit is heterogeneous particularly in pathological states. In such conditions, HbVs with a higher O_2 affinity should show a slower O_2 unloading that would be effective for oxygenating ischemic tissues.

In conclusion, HbVs provide the unique feature of allowing for the regulation of P_{50} by modulating the amount of coencapsulated PLP (33, 45). Recent studies showed the effectiveness of HBOCs with a lower P_{50} (higher O_2 affinity) as a means of implementing O_2 delivery targeted to ischemic tissue (2, 3, 41, 43). Thus this experimental method provides data useful for the design and optimization of O_2 carriers and suggests the possible utilization of HbVs for therapeutic approaches aimed at remedying ischemic conditions.

ACKNOWLEDGMENTS

The authors greatly acknowledge A. Barra and C. Walser (University of California-San Diego) for help with the animal preparations, Dr. S. Takeoka and Dr. K. Sou (Waseda University) for the preparation of the HbVs, and Dr. D. Erni (Inselspital University Hospital, Bern, ~~Germany~~ Switzerland) for meaningful discussions.

GRANTS

This study was supported in part by Health Sciences Research grants (Regulatory Science, Artificial Blood Project); the Ministry of Health, Labour and Welfare, Japan; Japan Society for the Promotion of Science Grant-In-Aid for Scientific Research B16300162; and National Heart, Lung, and Blood Institute Bioengineering Partnership Grant R24 HL-64395 and Grants R01 HL-40696 and R01 HL-62354. H. Sakai was an overseas research fellow of the Society of Japanese Pharmacopoeia.

REFERENCES

1. **Awasthi VD, Garcia D, Klipper R, Goins BA, and Phillips WT.** Neutral and anionic liposome-encapsulated hemoglobin: effect of postinserted poly(ethylene glycol)-distearoylphosphatidylethanolamine on distribution and circulation kinetics. *J Pharmacol Exp Ther* 309: 241–248, 2004.
2. **Baines AD, Adamson G, Wojciechowski P, Pliura D, Ho P, and Kluger R.** Effect of modifying O_2 diffusivity and delivery on glomerular and tubular function in hypoxic perfused kidney. *Am J Physiol Renal Physiol* 274: F744–F752, 1998.
3. **Baines AD and Ho P.** O_2 affinity of cross-linked hemoglobins modifies O_2 metabolism in proximal tubules. *J Appl Physiol* 95: 563–570, 2003.
4. **Buehler PW and Alayash AI.** Toxicities of hemoglobin solutions: in search of in-vitro and in-vivo model systems. *Transfusion* 44: 1516–1530, 2004.
5. **Chang TMS.** *Blood Substitutes: Principles, Methods, Products, and Clinical Trials.* Basel: Karger, 1997.
6. **Cabrales P, Sakai H, Tsai AG, Tsuchida E, and Intaglietta M.** Oxygen transport by low and normal P_{50} hemoglobin vesicles in extreme hemodilution. *Am J Physiol Heart Circ Physiol* 288: H1885–H1892, 2005. First published November 24, 2004; doi:10.1152/ajpheart.01004.2004.
7. **Contaldo C, Schramm S, Wettstein R, Sakai H, Takeoka S, Tsuchida E, Leunig M, Banic A, and Erni D.** Improved oxygenation in ischemic hamster flap tissue is correlated with increasing hemodilution with Hb vesicles and their O_2 affinity. *Am J Physiol Heart Circ Physiol* 285: H1140–H1147, 2003.
8. **Djordjevich L, Mayoral J, Miller IF, and Ivankovich AD.** Cardiorespiratory effects of exchange transfusions with synthetic erythrocytes in rats. *Crit Care Med* 15: 318–323, 1987.
9. **Duling BR and Berne RM.** Longitudinal gradients in periarteriolar oxygen tension. A possible mechanism for the participation of oxygen in the local regulation of blood flow. *Circ Res* 27: 669–678, 1970.
10. **Endrich B, Asaishi K, Gotz A, and Messmer K.** Technical report: a new chamber technique for microvascular studies inunanesthetized hamsters. *Res Exp Med (Berl)* 177: 125–134, 1980.
11. **Erni D, Wettstein R, Schramm S, Sakai H, Takeoka S, Tsuchida E, Leunig M, and Banic A.** Normovolemic hemodilution with hemoglobin-vesicle solution attenuates hypoxia in ischemic hamster flap tissue. *Am J Physiol Heart Circ Physiol* 284: H1702–H1709, 2003.
12. **Goda N, Suzuki K, Naito S, Takeoka S, Tsuchida E, Ishimura Y, Tamatani T, and Suematsu M.** Distribution of heme oxygenase isoform in rat liver: topographic basis for carbon monoxide-mediated micorvascular relaxation. *J Clin Invest* 101: 604–612, 1998.
13. **Intaglietta M, Johnson PC, and Winslow RM.** Microvascular and tissue oxygen distribution. *Cardiovasc Res* 32: 632–643, 1996.
14. **Intaglietta M, Silverman NR, and Tompkins WR.** Capillary flow velocity measurements in vivo and in situ by television methods. *Microvasc Res* 10: 165–179, 1975.
15. **Intaglietta M and Tompkins WR.** Microvascular measurements by video image shearing and splitting. *Microvasc Res* 5: 309–312, 1973.
16. **Izumi Y, Sakai H, Hamada K, Takeoka S, Yamahata Y, Kato R, Nishide H, Tsuchida E, and Kobayashi K.** Physiologic responses to exchange transfusion with hemoglobin vesicles as an artificial oxygen carrier in anesthetized rats: changes in mean arterial pressure and renal cortical tissue oxygen tension. *Crit Care Med* 24: 1869–1873, 1996.
17. **Kerger H, Torres Filho IP, Rivas M, Winslow RM, and Intaglietta M.** Systemic and subcutaneous microvascular oxygen tension in conscious Syrian golden hamsters. *Am J Physiol Heart Circ Physiol* 268: H802–H810, 1995.
18. **Kyokane Norimuzu S T, Tanial H, Yamaguchi T, Takeoka S, Tsuchida E, Naito M, Nimura Y, Ishimura Y, and Suematsu M.** Carbon monoxide from heme catabolism protects against hepatobiliary dysfunction in endotoxin-treated rat liver. *Gastroenterology* 120: 1227–1240, 2001.
19. **Linberg R, Conover CD, Shum KL, and Shorr RGL.** Increased tissue oxygenation and enhanced radiation sensitivity of solid tumors in rodents following polyethylene glycol conjugated bovine hemoglobin administration. In Vivo 12: 167–174, 1998.
20. **Lipowsky HH and Zweifach B.** Application of the "two slit" photometric technique to the measurement of microvascular volumetric flow rates. *Microvasc Res* 15: 93–101, 1978.
21. **McCarthy MR, Vandegeriff KD, and Winslow RM.** The role of facilitated diffusion in oxygen transport by cell-free hemoglobins: implications for the design of hemoglobin-based oxygen carriers. *Biophys Chem* 92: 103–117, 2001.
22. **Papenfuss HD, Gross JF, Intaglietta M, and Treese FA.** A transparent access chamber for the rat dorsal skin fold. *Microvasc Res* 18: 311–318, 1979.
23. **Richmond KN, Shonat RD, Lynch RM, and Johnson PC.** Critical P_{O_2} of skeletal muscle in vivo. *Am J Physiol Heart Circ Physiol* 277: H1831–H1840, 1999.
24. **Rudolph AS, Klipper RW, Goins B, and Phillips WT.** In vivo biodistribution of a radiolabelled blood substitute: ^{99m}Tc-labeled liposome-encapsulated hemoglobin in an anesthetized rabbit. *Proc Natl Acad Sci USA* 88: 10976–10980, 1991.
25. **Sakai H, Hara H, Tsai AG, Tsuchida E, Johnson PC, and Intaglietta M.** Changes in resistance vessels during hemorrhagic shock and resuscitation in conscious hamster model. *Am J Physiol Heart Circ Physiol* 276: H563–H571, 1999.
26. **Sakai H, Hara H, Yuasa M, Tsai AG, Takeoka S, Tsuchida E, and Intaglietta M.** Molecular dimensions of Hb-based O_2 carriers determine constriction of resistance arteries and hypertension in conscious hamster model. *Am J Physiol Heart Circ Physiol* 279: H908–H915, 2000.
27. **Sakai H, Hisamoto S, Fukutomi I, Sou K, Takeoka S, and Tsuchida E.** Detection of lipopolysaccharide in hemoglobin-vesicles by *Limulus amebocyte* lysate test with kinetic-turbidimetric gell clotting analysis and pretreatment with a surfactant. *J Pharm Sci* 93: 310–321, 2004.
28. **Sakai H, Horinouchi H, Tomiyama K, Ikeda E, Takeoka S, Kobayashi K, and Tsuchida E.** Hemoglobin-vesicles as oxygen carriers: influence on phagocytic activity and histopathological changes in reticuloendothelial systems. *Am J Pathol* 159: 1079–1088, 2001.
29. **Sakai H, Masada Y, Horinouchi H, Ikeda E, Sou K, Takeoka S, Suematsu M, Kobayashi K, and Tsuchida E.** Physiologic capacity of reticuloendothelial system for degradation of hemoglobin-vesicles (artificial oxygen carriers) after massive intravenous doses by daily repeated infusion for 14 days. *J Pharmacol Exp Ther* 311: 874–884, 2004.
30. **Sakai H, Masada Y, Horinouchi H, Yamamoto M, Ikeda E, Takeoka S, Kobayashi K, and Tsuchida E.** Hemoglobin-vesicles suspended in recombinant human serum albumin for resuscitation from hemorrhagic shock in anesthetized rats. *Crit Care Med* 32: 539–545, 2004.

31. **Sakai H, Suzuki Y, Kinoshita M, Takeoka S, Maeda N, and Tsuchida E.** O_2-release from Hb-vesicles evaluated using an artificial narrow O_2-permeable tube: comparison with RBC and acellular Hb. *Am J Physiol Heart Circ Physiol* 285: H2543–H2551, 2003.
32. **Sakai H, Takeoka S, Yokohama H, Seino Y, Nishide H, and Tsuchida E.** Purification of concentrated Hb using organic solvent and heat treatment. *Protein Expr Purif* 4: 563–569, 1993.
33. **Sakai H, Tsai AG, Rohlfs RJ, Hara H, Takeoka S, Tsuchida E, and Intaglietta M.** Microvascular responses to hemodilution with Hb-vesicles as red blood cell substitutes: influences of O_2 affinity. *Am J Physiol Heart Circ Physiol* 276: H553–H562, 1999.
34. **Sakai H, Yuasa M, Onuma H, Takeoka S, and Tsuchida E.** Synthesis and physicochemical characterization of a series of hemoglobin-based oxygen carriers: objective comparison between cellular and acellular types. *Bioconjug Chem* 11: 56–64, 2000.
35. **Shibata M, Ichioka S, Ando J, and Kamiya A.** Microvascular and interstitial P_{O_2} measurements in rat skeletal muscle by phosphorescence quenching. *J Appl Physiol* 91: 321–327, 2001.
36. **Shirasawa T, Izumizaki M, Suzuki YI, Ishihara A, Shimizu T, Tamaki M, Huang F, Koizumi KI, Iwase M, Sakai H, Tsuchida E, Ueshima U, Inoue H, Koseki H, Senda H, Kuriyama T, and Homma I.** Oxygen affinity of hemoglobin regulates O_2 consumption, metabolism, and physical activity. *J Biol Chem* 278: 5035–5043, 2003.
37. **Sou K, Naito Y, Endo T, Takeoka S, and Tsuchida E.** Effective encapsulation of proteins into size-controlled phospholipid vesicles using freeze-thawing and extrusion. *Biotechnol Progr* 19: 1547–1552, 2003.
38. **Takeoka S, Teramura Y, Atoji T, and Tsuchida E.** Effect of Hb-encapsulation with vesicles on H_2O_2 reaction and lipid peroxidation. *Bioconjug Chem* 13: 1302–1308, 2002.
39. **Tomson FN and Wardrop KJ.** Clinical chemistry and hematology. In: *Laboratory Hamsters*, edited by van Hoosier GL Jr and McPherson CW. Orlando, FL: Academic, 1987, chapt. 3. AQ: 2
40. **Torres Filho IP and Intaglietta M.** Microvascular P_{O_2} measurements by phosphorescence decay method. *Am J Physiol Heart Circ Physiol* 265: H1434–H1438, 1993.
41. **Tsai AG, Kerger H, and Intaglietta M.** Microcirculatory consequences of blood substitutution with αα-hemoglobin. In: *Blood Substitutes: Physiological Basis of Efficacy*, edited by Winslow RM, Vandegriff K, and Intaglietta M. Boston, MA: Birkhauser, 1995, p. 155–174.
42. **Tsai AG, Friesenecker B, Mazzoni MC, Kerger H, Buerk DG, Johnson PC, and Intaglietta M.** Microvascular and tissue oxygen gradients in the rat mesentery. *Proc Natl Acad Sci USA* 95: 6590–6595, 1998.
43. **Tsai AG, Vandegriff KD, Intaglietta M, and Winslow RM.** Targeted O_2 delivery by low-P_{50} hemoglobin: a new basis for O_2 therapeutics. *Am J Physiol Heart Circ Physiol* 285: H1411–H1419, 2003.
44. **Vanderkool JM, Maniara G, Green TJ, and Wilson DF.** An optical method for measurement of dioxygen concentration based on quenching of phosphorescence. *J Biol Chem* 262: 5476–5482, 1987.
45. **Wang L, Morizawa K, Tokuyama S, Satoh T, and Tsuchida E.** Modulation of oxygen-carrying capacity of artificial red cells (ARC). *Polymer Adv Technol* 4: 8–11, 1992.

LIPPINCOTT WILLIAMS & WILKINS

Critical Care Medicine

OFFICIAL JOURNAL OF THE SOCIETY OF CRITICAL CARE MEDICINE

Title: New generation of hemoglobin-based oxygen carriers evaluated for oxygenation of critically ischemic hamster flap tissue

Author(s): Claudio Contaldo MD; Jan Plock MD; Hiromi Sakai PhD; Shinji Takeoka PhD; Eishun Tsuchida PhD; Michael Leunig MD; Andrej Banic MD, PhD; Dominique Erni MD

Objectives: The aim of this study was to investigate and compare the effects of a traditionally formulated, low-viscosity, right-shifted polymerized bovine hemoglobin solution and a highly viscous, left-shifted hemoglobin vesicle solution (HbV-HES) on the oxygenation of critically ischemic peripheral tissue.

Design: Randomized, prospective study.

Setting: University laboratory.

Subject: A total of 40 male golden Syrian hamsters.

Interventions: Island flaps were dissected from the back skin of anesthetized hamsters. The flap included a critically ischemic, hypoxic area that was perfused via a collateralized vasculature. One hour after completion of the preparation, the animals received a 33% blood exchange with 6% hydroxyethyl starch 200/0.5 (HES, n = 9), HbV suspended in HES (HbV-HES, n = 8), or polymerized bovine hemoglobin solution (n = 9).

Measurements and Main Results: Three hours after the blood exchange, microcirculatory blood flow (laser-Doppler flowmetry) was increased to 262% of baseline for HbV-HES ($p < .01$) and 197% for polymerized bovine hemoglobin solution ($p < .05$ vs. baseline and HbV-HES). Partial tissue oxygen tension (bare fiber probes) was only improved after HbV-HES (9.4 torr to 14.2 torr, $p < .01$ vs. baseline and other groups). The tissue lactate/pyruvate ratio (microdialysis) was elevated to 51 in the untreated control animals, and to 34 ± 8 after HbV-HES ($p < .05$ vs. control) and 38 ± 11 after polymerized bovine hemoglobin solution (not significant).

Conclusions: Our study suggests that in critically ischemic and hypoxic collateralized peripheral tissue, oxygenation may be improved by

normovolemic hemodilution with HbV-HES. We attributed this improvement to a better restoration of the microcirculation and oxygen delivery due to the formulation of the solution.

Exchange transfusion with entirely synthetic red-cell substitute albumin-heme into rats: Physiological responses and blood biochemical tests

Yubin Huang,[1] Teruyuki Komatsu,[1] Hisashi Yamamoto,[2] Hirohisa Horinouchi,[3] Koichi Kobayashi,[3] Eishun Tsuchida[1]

[1]*Advanced Research Institute for Science and Engineering, Waseda University,3-4-1 Okubo, Shinjuku, Tokyo 169-8555, Japan*

[2]*Pharmaceutical Research Center, NIPRO Corporation, 3023 Nojimachi, Kusatsu, Shiga 525-0055, Japan*

[3]*Department of General Thoracic Surgery, School of Medicine, Keio University,35 Shinanomachi, Shinjuku, Tokyo 160-8582, Japan*

Received 24 October 2003; revised 13 May 2004; accepted 2 June 2004
Published online 5 August 2004 in Wiley InterScience (www.interscience.wiley.com). DOI: 10.1002/jbm.a.30127

Abstract: Recombinant human serum albumin (rHSA) incorporating 2-[8-{*N*-(2-methylimidazolyl)}octanoyloxymethyl]-5,10,15,20-[tetrakis{α,α,α,α-*o*-(1-methylcyclohexanoyl)amino}-phenyl]porphinatoiron(II) [albumin-heme (rHSA-heme)] is an artificial hemoprotein which has the capability to transport O_2 *in vitro* and *in vivo*. A 20% exchange transfusion with rHSA-heme into anesthetized rats has been performed to evaluate its clinical safety by monitoring the circulation parameters and blood parameters for 6 h after the infusion. Time course changes in all parameters essentially showed the same features as those of the control group (without infusion) and rHSA group (with administration of the same amount of rHSA). Blood biochemical tests of the withdrawn plasma at 6 h after the exchange transfusion have also been carried out. No significant difference was found between the rHSA-heme and rHSA groups, suggesting the initial clinical safety of this entirely synthetic O_2-carrier as a red-cell substitute. © 2004 Wiley Periodicals, Inc. J Biomed Mater Res 71A: 63–69, 2004

Key words: exchange transfusion; entirely synthetic red-cell substitute; albumin-heme; blood biochemical tests; O_2 carrier.

INTRODUCTION

Although hemoglobin (Hb)-based O_2 carriers are currently undergoing clinical trials as red-cell substitutes or oxygen therapeutics, there are still some concerns about new infectious pathogens in Hb and unresolved side effects such as vasoconstriction.[1–4] Recombinant human serum albumin (rHSA) incorporating the synthetic heme albumin-heme is an artificial hemoprotein that has the potential to bind and release O_2 under physiological conditions in the same manner as Hb and myoglobin.[5–7] In fact, the albumin-heme can transport O_2 through the body and release O_2 to tissues as a red-cell substitute without any acute side effects.[8,9] For example, rHSA including four molecules of 2-[8-{*N*-(2-methylimidazolyl)}-octanoyloxymethyl]-5,10,15,20-[tetrakis{α,α,α,α-*o*-(1-methylcyclohexanoyl)amino}phenyl]porphinatoiron(II) (Scheme 1) is one of the promising materials.[7] Recent study on the 30% exchange transfusion with rHSA-heme after 70% hemodilution with 5 wt % rHSA with the use of anesthetized rats demonstrated that the administration of this material improved the circulatory volume and resuscitated the hemorrhagic shock state.[10] The declined MAP and the mixed venous partial O_2 pressure immediately recovered, and the lowered renal cortical O_2-pressure also significantly increased.

In order to evaluate the initial clinical safety of this albumin-based O_2-carrier, a 20% exchange transfusion with rHSA-heme into anesthetized rats was performed, and the time courses of the circulation parameters (MAP, HR, respiration rate) and blood parameters (paO_2, pvO_2, pH, blood cell numbers) were measured for 6 h, which is adequate time to determine acute toxicity. Blood biochemical tests of the withdrawn plasma were also been carried out.

MATERIALS AND METHODS

Preparation of rHSA-heme

Recombinant human serum albumin (rHSA, Albrec®, 25 wt %) was obtained from the NIPRO Corp. (Osaka). The 5

Correspondence to: E. Tsuchida; e-mail: eishun@waseda.jp
Contract grant sponsor: MHLW
Contract grant sponsor: JSPS; contract grant number: 16350093
Contract grant sponsor: MEXT; contract grant number: 16655049

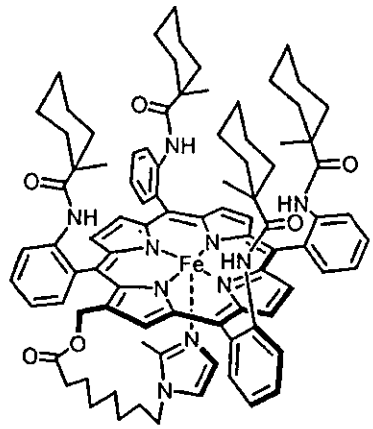

Scheme 1

g/dL rHSA was made by diluting Albrec® with saline solution (Otsuka Pharmaceutical Co., Ltd.). The rHSA-heme solution ([rHSA]: 4.9 g/dL, pH 7.45, [heme]: 2.8 m*M*, O_2-binding affinity ($p_{1/2}O_2$): 37 Torr) used for the experiments was prepared according to a previously reported procedure.[11] The red-colored rHSA-heme solution was filtered with the use of DISMIC 25CS045AS just before use.

Exchange transfusion

The investigations were carried out with 18 male Wister rats (305±3.6 g). The animals were placed on the heating pad under an inhalation anesthesia with sevofluran; its concentration was kept 2.0% for the operations and 1.5% for the experiments. After incision was made in the neck, the heparinized catheter (Natsume Seisakusho SP-55) was introduced into the right common carotid artery for blood withdrawal. Other catheters (SP-31) were inserted into the left femoral artery for a continuous MAP monitoring, and the right femoral vein for sample injection.

After stabilization of the animal condition, the 20% exchange transfusion (total blood volume of rat was estimated to be 64 mL/kg weight) was performed by 1 mL blood withdrawal via the common carotid artery and 1 mL rHSA-heme infusion from the femoral vein (each 1 mL/min) with four repeating cycles (n = 6, rHSA-heme group). Blood was taken from the artery (0.3 mL) and vein (0.2 mL) at the following five points; (i) before, (ii) immediately after, (iii) 1 h after, (iv) 3 h after, and (v) 6 h after the exchange transfusion. MAP and HR were recorded with the use of a polygraph system (NIHON KODEN LEG-1000 Ver. 01-02 or PEG-1000 Ver. 01-01) at the same time point as stated above. Withdrawn blood was rapidly applied to a blood gas system (Radio Meter Trading ABL555) to obtain the O_2-pressure (paO_2) and pH for the arterial blood, and the O_2-pressure (pvO_2) for the venous blood. The blood cell numbers were counted by a multisystem automatic blood cell counter (Sysmex KX-21). After 6 h, 4 mL of the venous blood was taken for each animal before sacrifice by sodium pentobarbital overdose. The blood samples were centrifuged at 4°C (Beckman Coulter Co., Optima LE-80K for 3500 × rpm, 10 min), and the plasma phase was frozen (−20°C) for blood biochemical tests. As a reference group, the 5 g/dL rHSA solution was administered similarly into rats (n = 6, rHSA group). Furthermore, six rats without infusion (operation only) were also set as a control group.

All animal handling and care was in accordance with the NIH guidelines. The protocol details were approved by the Animal Care and Use Committee of Keio University.

Blood biochemical tests

A total of 30 analytes, that is, total protein (TP), albumin (Alb), albumin/globulin ratio (A/G), aspartate aminotransferase (AST), alanine aminotransferase (ALT), lactate dehydrogenase (LDH), alkaline phosphatase (ALP), γ-glutamyltransferase (γ-GTP), leucine aminopeptidase (LAP), choline esterase (ChE), total bilirubin (TBil), direct bililubin (DBil), creatinine (CRN), blood urea nitrogen (BUN), uric acid (UA), amylase, lipase, creatine phosphokinase (CPK), total cholesterol (TCho), free cholesterol (FCho), cholesterol ester (ECho), β-lipoprotein (β-LP), high-density lipoprotein (HDL)-cholesterol, neutral fat (triglyceride, TG), total lipid, free fatty acid (FFA), phospholipids (PhL), K^+, Ca^{2+} and Fe^{3+}, were measured by Kyoto Microorganism Institute (Kyoto).

Data analysis

MAP, HR, respiration rate, paO_2 and pvO_2 were represented as percent ratios of the basal values with mean ± standard error of mean (SEM). Body temperature, pH, blood cell numbers and the data of blood biochemical tests were shown as mean ± SEM.

Statistical analysis were performed by repeated-analysis measures of variance (ANOVA) followed by the paired t-test for comparison with a basal value (body temperature), by the Bartlett test followed by the Tukey-Kramer multiple comparison test for pH, blood cell numbers, and the results of the blood biochemical tests, and by the Kruskal-Wallis test followed by the Tukey-Kramer multiple comparison test for more than three groups (MAP, HR, respiration rate, paO_2, and pvO_2). Values of $p < 0.05$ were considered significant. The statistical analytical software used was StatView (SAS Institute, Inc.).

RESULTS

Circulation parameters

The basal values of some measurements, the data values of which are represented by percent ratios, are summarized in Table I. There are no significant differences between the three groups (control, rHSA, and rHSA-heme groups).

The body temperature of each group was constantly

TABLE I
Basal Values of Each Group

	Control	rHSA	rHSA-heme
MAP (mmHg)	99 ± 2.8	101 ± 2.8	100 ± 6.1
HR (beats/min)	404 ± 19	435 ± 19	420 ± 13
Respiration rate (breaths/min)	66 ± 0.7	75 ± 4.0	70 ± 2.1
paO_2 (mmHg)	84.7 ± 3.1	84.9 ± 3.7	80.8 ± 2.2
pvO_2 (mmHg)	51.0 ± 1.5	45.7 ± 1.1	51.0 ± 1.7
Body weight (g)	305 ± 4.0	304 ± 2.8	305 ± 4.1

maintained within 36.9–37.4°C during the experiments [Fig. 1(a)].

The MAP time course in the control group demonstrated only a small deviation within 83.8–100.0% for 6 h. In the rHSA and rHSA-heme groups, the observed changes in MAP were almost the same as those of the control group. They ranged within 93.2–100 and 89.3–100%, respectively. It is remarkable that no vasoactive reaction was seen after the infusion of rHSA-heme [Fig. 1(b)].

The HR of the control, rHSA, and rHSA-heme groups remained unaltered for 6 h. The values of the control, rHSA, and rHSA-heme groups were in the range of 98.3–103.9, 96.9–108.8, and 85.7–100.0%, respectively [Fig. 1(c)].

The respiration rates also remained stable during the measurements. No significant difference was recognized among the three groups [Fig. 1(d)].

Blood-gas parameters

No difference in the pH changes was observed in the three groups. The pH values of the control, rHSA, and rHSA-heme groups were constant in the narrow ranges of 7.42–7.45, 7.42–7.44, and 7.42–7.44, respectively [Fig. 2(a)].

The paO_2 values of the control, rHSA, and rHSA-heme groups were also constant in the range of 100–108.1, 100–109.1, and 100–110.8%, respectively, by the end of measurements [Fig. 2(b)].

The pvO_2 of the control, rHSA and rHSA-heme groups demonstrated only small changes within 81.5–100.0, 84.9–108.4, and 81.9–100.0%, respectively [Fig. 2(c)].

Blood cell numbers

The Hct values of the control group were unchanged from 34.8–37.0% during the experiment. On the other hand, the 20% exchange transfusion with the

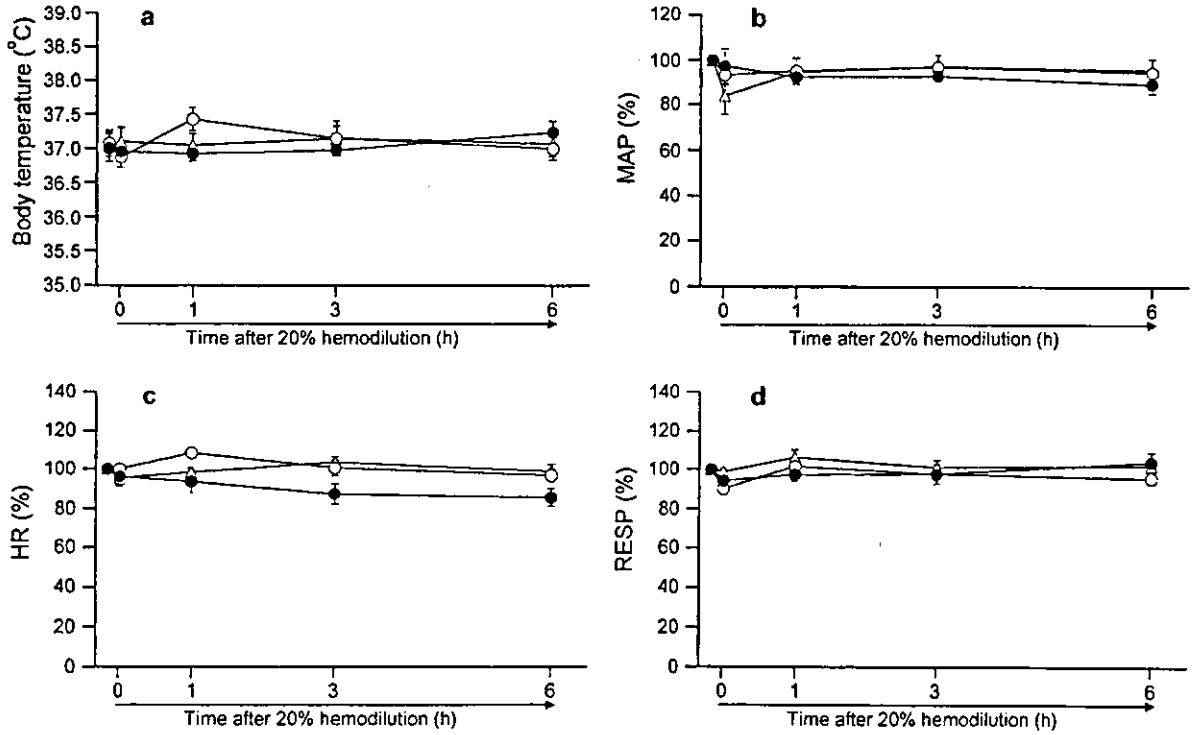

Figure 1. (a) Time courses of body temperature, (b) mean arterial pressure (MAP), (c) heart rate (HR), and (d) respiration rate (RESP) in anesthetized rats after 20% exchange transfusion with rHSA-heme or rHSA solution. Each value represents the mean ± SEM of six rats (triangles, control group without infusion; open circles, rHSA group; solid circles, rHSA-heme group).

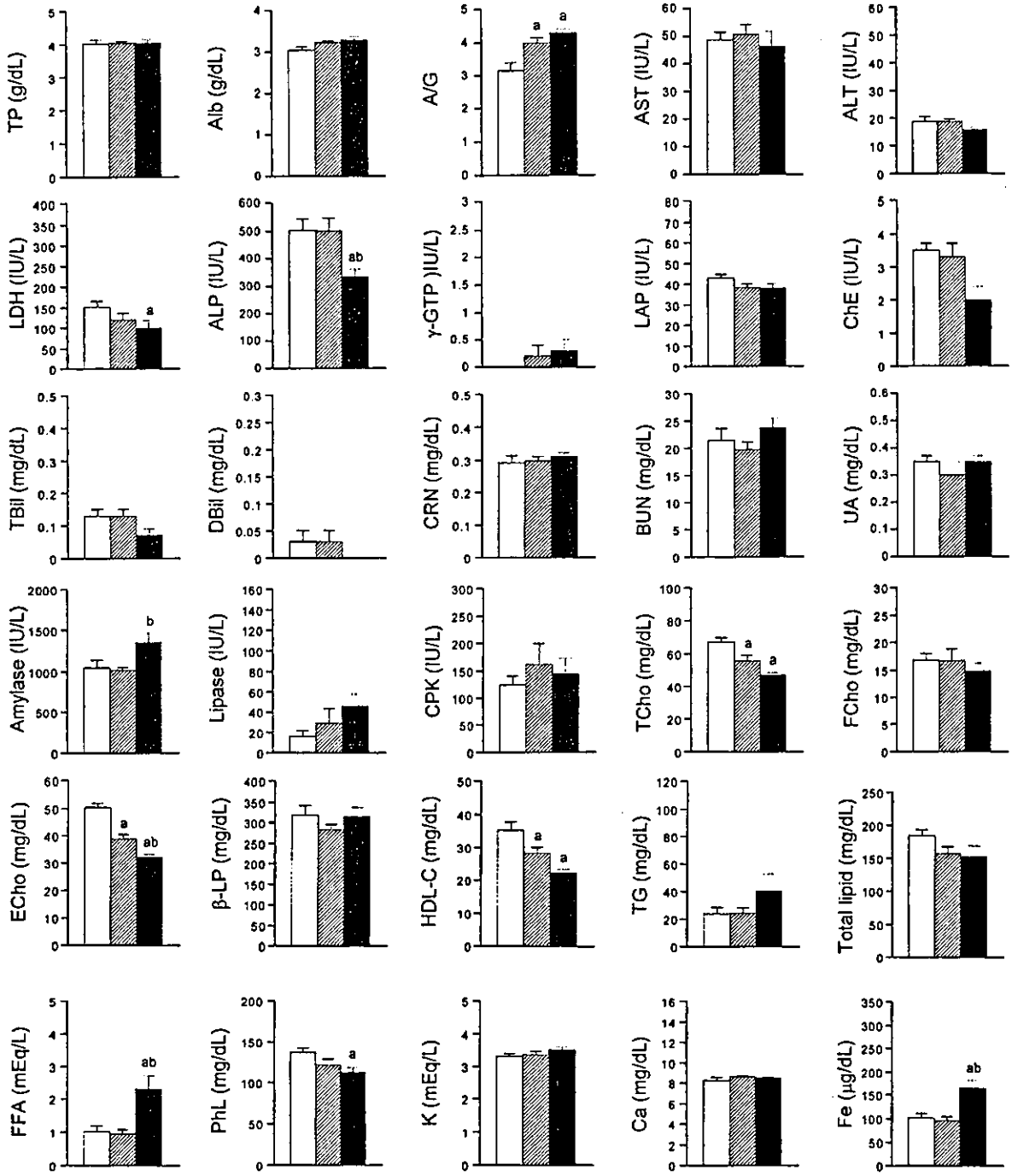

Figure 4. Blood biochemical tests of rat plasma after 20% exchange transfusion with rHSA-heme or rHSA solution. Each value represents the mean ± SEM of six rats (white bar, control group without infusion; diagonal bar, rHSA group; black bar, rHSA-heme group). $^{a}p < 0.05$ versus control group (Tukey-Kramer test); $^{b}p < 0.05$ versus rHSA group (Tukey-Kramer test).

with rHSA-heme. These results showed the initial clinical safety of the rHSA-heme solution, which allows us to undergo further advanced preclinical testing of this synthetic O_2-carrying hemoprotein as a new class of red-cell substitutes. Biochemical tests and histopathological observations for 7 days after the exchange transfusion with rHSA-heme will be reported in a forthcoming article.

The authors are grateful to Dr. Toshiya Kai (NIPRO Corp.) for preparation and characterizations of the albumin-heme solutions. They also thank Dr. Ichiro Hirotsu

(NIPRO Corp.) for his useful discussions and valuable suggestions on the experimental results. This work was partially supported by Health Science Research Grants (Research on Pharmaceutical and Medical Safety) of the MHLW, Grant-in-Aid for Scientific Research (No. 16350093) from JSPS, and Grant-in-Aid for Exploratory Research (No. 16655049) from MEXT.

References

1. Chang TMS. Recent and future developments in modified hemoglobin and microencapsulated hemoglobin as red blood cell substitutes. Artif Cells Blood Substit Immobil Biotechnol 1997;25:1–24.
2. Tsuchida E. Perspectives of blood substitutes. In: Tsuchida E, editor. Blood substitutes: Present and future perspectives. Lausanne: Elsevier; 1998. p 1–14.
3. Winslow RM. New transfusion strategies: red cell substitutes. Annu Rev Med 1999;50:337–353.
4. Squires JE. Artificial blood. Science 2002;295:1002–1005.
5. Komatsu T, Hamamatsu K, Wu J, Tsuchida E. Physicochemical properties and O_2-coordination structure of human serum albumin incorporating tetrakis(*o*-pivamido)phenylporphyrinatoiron(II) Derivatives. Bioconjug Chem 1999;10:82–86.
6. Tsuchida E, Komatsu T, Matsukawa Y, Hamamatsu K, Wu J. Human serum albumin incorporating tetrakis(*o*-pivalamido-)phenylporphinatoiron(II) derivative as a totally synthetic O_2-carrying hemoprotein. Bioconjug Chem 1999;10:797–802.
7. Komatsu T, Matsukawa Y, Tsuchida E. Effect of heme structure on O_2-binding properties of human serum albumin–heme hybrids: intramolecular histidine coordination provides a stable O_2-adduct complex. Bioconjug Chem 2002;13:397–402.
8. Tsuchida E, Komatsu T, Hamamatsu K, Matsukawa Y, Tajima A, Yoshizu A, Izumi Y, Kobayashi K. Exchange transfusion of albumin-heme as an artificial O_2-infusion into anesthetized rats: physiological responses, O_2-delivery and reduction of the oxidized hemin sites by red blood cells. Bioconjug Chem 2000;11:46–50.
9. Tsuchida E, Komatsu T, Matsukawa Y, Nakagawa A, Sakai H, Kobayashi K, Suematsu M. Human serum albumin incorporating synthetic heme: red blood cell substitute without hypertension by nitric oxide scavenging. J Biomed Mater Res 2003; 64A:257–261.
10. Komatsu T, Yamamoto H, Huang Y, Horinouchi H, Kobayashi K, Tsuchida E. Physiological responses to exchange transfusion with synthetic oxygen-carrier "albumin-heme" in acute anemia after 70% hemodilution. J Biomed Mater Res. Submitted for publication.
11. Huang Y, Komatsu T, Nakagawa A, Tsuchida E, Kobayashi S. Compatibility *in vitro* of albumin-heme (O_2-carrier) with blood cell components. J Biomed Mater Res 2003;66A:292–297.
12. Gorelick FS. Acute pancreatitis. In: Yamada T, editor. Textbook of gastroenterology (2nd ed.). Philadelphia: Lippincott; 1955. p 2064–2091.
13. Agarwal N, Pitchumoni CS, Sivaprasad AV. Evaluating tests for acute pancreatitis. Am J Gastroenterol 1990;85:356–361.
14. Clavin PA, Burgan S, Moossa AR. Serum enzyme and other laboratory tests in acute pancreatitis. Br J Surg 1989;76:1234–1238.

ARTICLE

OBC

www.rsc.org/obc

Synthesis of protoheme IX derivatives with a covalently linked proximal base and their human serum albumin hybrids as artificial hemoprotein

Akito Nakagawa, Naomi Ohmichi, Teruyuki Komatsu and Eishun Tsuchida*

Advanced Research Institute for Science and Engineering, Waseda University, 3-4-1 Ohkubo, Shinjuku-ku, Tokyo 169-8555, Japan. E-mail: eishun@waseda.jp; Fax: +81 3-3205-4740; Tel: +81 3-5286-3120

Received 15th June 2004, Accepted 3rd September 2004
First published as an Advance Article on the web 27th September 2004

The simple one-pot reaction of protoporphyrin IX and ω-(*N*-imidazolyl)alkylamine or *O*-methyl-L-histidyl-glycine with benzotriazol-1-yl-oxytris(dimethylamino)phosphonium hexafluorophosphate at room temperature produced a series of protoporphyrin IX species with a covalently linked proximal base at the propionate side-chain. The central iron was inserted by the general $FeCl_2$ method, converting the free-base porphyrins to the corresponding protoheme IX derivatives. Mesoporphyrin IX and diacetyldeuteroporphyrin IX analogues were also prepared by the same procedure. The Fe(II) complexes formed dioxygen (O_2) adducts in dimethylformamide at 25 °C. Some of them were incorporated into the hydrophobic domain of recombinant human serum albumin (rHSA), providing albumin–heme hybrids (rHSA–heme), which can bind and release O_2 in aqueous media (pH 7.3, 25 °C). The oxidation process of converting the dioxygenated heme in rHSA to the inactive Fe(III) state obeyed first-order kinetics, indicating that the μ-oxo dimer formation was prevented by the immobilization of heme in the albumin scaffold. The rHSA–heme, in which the histidylglycil tail coordinates to the Fe(II) center, showed the most stable O_2 adduct complexes.

Introduction

Numerous model compounds of hemoglobin (Hb) and myoglobin (Mb) have already been prepared and their O_2-binding equilibria and kinetics were extensively studied.[1] In particular, synthetic hemes having a sterically encumbered porphyrin platform can form stable O_2 adducts in organic solvent at room temperature. If we are to reproduce or mimic any biochemical reaction, the aqueous medium is particularly important. The dioxygenated complexes of highly-modified hemes are unfortunately oxidized to the ferric state in water. Human serum albumin (HSA) is the most abundant plasma protein in our circulatory system and solubilizes hydrophobic small molecules.[2] We have found that synthetic hemes are also spontaneously incorporated into HSA, which provides unique albumin–heme hybrids (HSA–hemes) and allows their Fe(II) states to remain stable in aqueous solution.[3] Actually, recombinant HSA[4] (rHSA) including tetrakis(α,α,α,α-*o*-pivalamidophenyl)porphinatoiron(II) with a covalently linked proximal base can reversibly bind and release O_2 under physiological conditions, and acts as an artificial O_2 transporter in the blood stream.[5] Our next target is to realize O_2 coordination to rHSA–heme involving protoheme IX in the same manner as natural Hb and Mb. The dioxygenation of protoheme IX has several advantages. (1) Synthetic procedures are rather simplified with respect to the highly modified tetraphenylporphyrin. (2) It has the same structure and thus the same spectra as do hemoproteins; this makes possible the study of subtle changes in the protein nanostructure. (3) Its metabolism process has been clarified,[6] which is an advantage for medical use as an artificial O_2 carrier.

We report herein the simple synthetic methodology of protoheme IX derivatives with a covalently-linked proximal imidazolyl arm and the O_2-binding properties of the obtained rHSA–hemes.

Results and discussion

Synthesis

The free-base porphyrins with a covalently linked proximal base (**1a–8a**, Scheme 1) were synthesized by the one-pot reaction of protoporphyrin IX, ω-(*N*-imidazolyl)alkylamine [R_2H; 3-(*N*-imidazolyl)propylamine, 4-(*N*-(2-methylimidazolyl))-butylamine or *O*-methyl-L-histidyl-glycine] for one propionic acid group, and a capping alcohol or amine on the other side (R_3H; MeOH, EtOH or $MeNH_2$) in the presence of benzotriazol-1-yl-oxytris(dimethylamino)phosphonium hexafluorophosphate (BOP) at 25 °C in pyridine [or dimethylformamide (DMF)] (Scheme 2). The carbonyl attachment was made through either an ester or an amide function. After the reaction, the mixture was poured into 10% NaCl solution, which led to the precipitation of the crude porphyrin. Centrifugation at 7000 g for 30 min gave a purple pellet. The pyridine (or DMF), BOP, R_2H and R_3H in the supernatant were all discarded at this point. The obtained precipitate was dissolved in $CHCl_3$ and showed several spots on a thin layer chromatograph. The anpolar band corresponds to the double R_3-substituted component (ex. protoporphyrin IX diethyl ester in the cases of **2**, **5**, **6**) and the second band is the desired porphyrin, which is purified by a silica gel chromatographic separation (yield: 20–30%). The iron was then inserted by the general $FeCl_2$ method with 2,6-lutidine in DMF solution, giving the corresponding hemins. Mesoporphyrin IX and diacetyldeuteroporphyrin IX also gave similar analogues (**7b** and **8b**). We obtained a mixture of two isomeric compounds that we were unable to separate.

Traylor and co-workers reported many pioneering studies on "chelated hemes".[7] They synthesized compound **1b**, for instance, using an acid anhydride procedure directly from protohemin chloride.[7c] First, the protohemin dimethyl ester was partially hydrolyzed and, after purification, the mono acid was coupled to a 3-(*N*-imidazolyl)propylamine by the pivaloyl chloride method. Nevertheless, reaction mixtures involving the diacid and monoacid are normally insoluble in common organic solvents, therefore, the yield of this reaction largely depends on the separation techniques. In contrast, our simple procedure makes it possible to synthesize a series of new protoporphyrins with a wide variety of proximal bases and end-capping groups of the other propionic acid.

Dioxygenation of heme in DMF solution

The obtained hemin complexes **1b–8b** in DMF solution were reduced to the corresponding Fe(II) complexes using a solution

DOI: 10.1039/b409017a

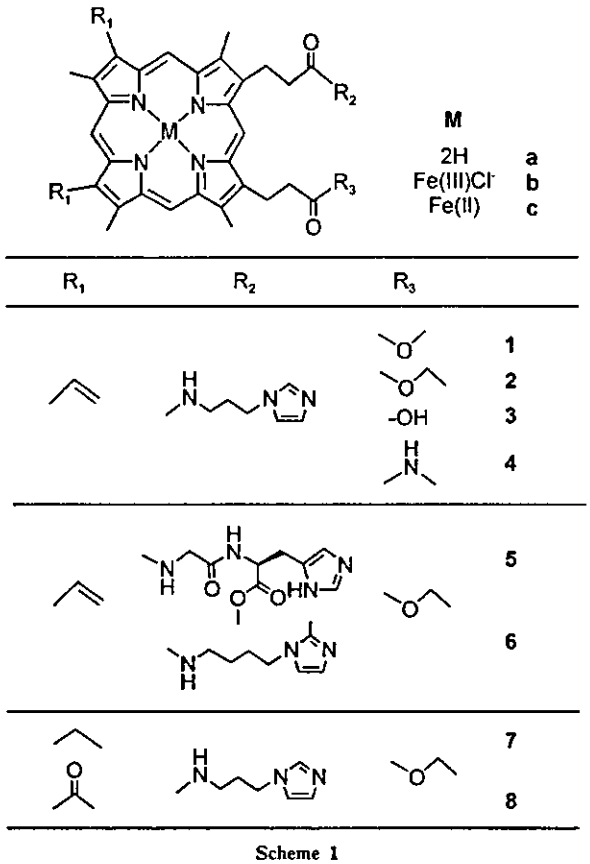

Scheme 1

of the crown ether-dithionite as reducing agent.[8] The UV-vis absorption spectrum of **2c** [Fe(II) complex] under a nitrogen (N_2) atmosphere showed a single broad band in the α,β region around 520–580 nm. This indicates the formation of a typical five-*N*-coordinate high-spin complex,[7] in which the proximal imidazole group intramolecularly coordinates to the central Fe(II) ion in the non-coordinating solvent (DMF) (Fig. 1). Because 2-methyl-imidazole significantly inhibits a sixth ligand binding to the *trans*-position, **6c** also demonstrated a similar 5-coordinated spectrum in DMF solution. Upon bubbling of the O_2 gas through the solution of **2c**, the spectral pattern immediately changed to that of the O_2 adduct complex. After adding carbon monoxide (CO) gas, the heme changed to a very stable carbonyl complex. Similar absorption changes were observed for all the heme derivatives, **1c–8c**. The absorption maxima (λ_{max}) of compounds **1c–8c** in DMF solution under N_2, O_2 and CO atmospheres are summarized in Table 1.

The positions and the relative intensities of all peaks were independent of the temperature changes from 5 to 25 °C. In general, the electron density of the porphyrin ring systematically changes the λ_{max} of the B-band and Q-band.[9] The replacement of the vinyl groups at the 3,8-positions of protoheme IX with ethyl groups (from **2c** to **7c**) produced a hypsochromic shift. In contrast, changing the vinyl groups to electron withdrawing acetyl groups (from **2c** to **8c**) produced a bathochromic shift.

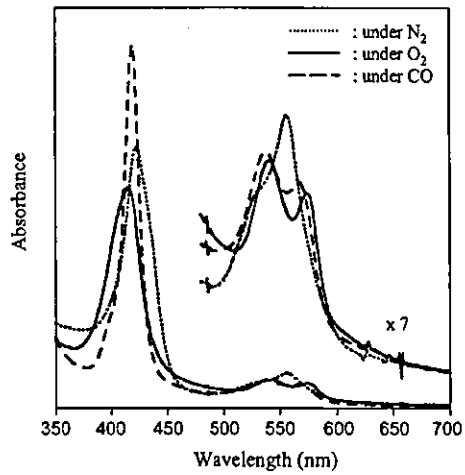

Fig. 1 UV-vis spectra of **2c** in DMF at 25 °C.

Table 1 Absorption maxima (λ_{max}) of heme derivatives in DMF under various conditions

	λ_{max}/nm		
Compound	Under N_2	Under O_2	Under CO
1c (15 °C)	427, 530, 558	414, 543, 575	420, 540, 569
1c (25 °C)	424, 532, 559	412, 542, 575	420, 539, 567
2c (5 °C)	422, 531, 556	415, 541, 574	419, 537, 567
2c (25 °C)	421, 533, 557	409, 539, 571	418, 537, 565
3c (25 °C)	426, 537, 559	415, 543, 575	420, 539, 567
4c (5 °C)	421, 527, 555	413, 540, 572	417, 536, 564
5c (5 °C)	419, 529, 551	406, 537, 569	412, 534, 562
5c (25 °C)	423, 533, 557	408, 539, 573	419, 538, 567
6c (5 °C)	430, 555	413, 547, 576	418, 538, 561
7c (25 °C)	414, 523, 548	407, 531, 563	409, 529, 556
8c (5 °C)	440, 541, 571	432, 552, 579	434, 549, 576
8c (25 °C)	439, 545, 569	431, 552, 580	433, 548, 577

We could not find any significant difference in the absorption maxima of **1c–6c**, because modification of the propionic acids did not affect the electron density of the porphyrin macrocycle.

Preparation of rHSA–heme

Aqueous solutions of rHSA–heme were prepared by injecting an ethanol solution of the carbonylated heme into an aqueous solution of rHSA. The inclusion of heme into rHSA was confirmed by the following results: (1) Sepharose gel column chromatography showed the elution peaks of heme and rHSA coincided at the same position, (2) during dialysis of the rHSA–heme solution against phosphate buffer, the outer aqueous phase did not contain the heme component. The UV-vis absorption spectra of the obtained solution showed that the heme was retained as a CO adduct complex.

The binding number of heme in one rHSA was determined to be 0.9–1.1 (mol/mol) by assaying the iron and rHSA concentrations. The binding constant of **1b** for rHSA was estimated to be *ca.* 4×10^6 M^{-1}, which is approximately 1/25 of that for protohemin IX itself to albumin (*ca.* 1×10^8 M^{-1}).[10] Polar heme derivatives **3c** with monopropionic acid and **4c** with a methyl-

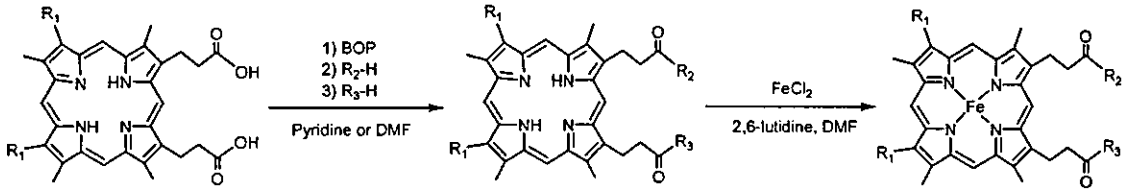

BOP: benzotriazol-1-yl-oxytris(dimethylamino)phosphonium hexafluorophosphate

Scheme 2 Synthesis of protoheme IX derivatives.

Table 2 Absorption maxima (λ_{max}) of rHSA–hemes in phosphate buffer solution (pH 7.3) at 25 °C

Compounds	λ_{max}/nm		
	Under N_2	Under O_2	Under CO
rHSA–1c	420, 536, 561	414, 540, 567	419, 541, 566
rHSA–2c	420, 538, 561	416, 540, 567	421, 543, 567
rHSA–5c	422, 539, 561	418, 540, 571	422, 541, 569
rHSA–8c	444, 549, 571	432, 551, 580	440, 555, 578

amide capping group at the porphyrin periphery were partially oxidized to the Fe(III) state during the inclusion process. Since the binding force of the heme derivative to rHSA is a hydrophobic interaction,[11] relatively polar porphyrins may not be incorporated into a certain domain of rHSA and easily oxidized compared to more apolar ones.

The circular dichroism spectra of the rHSA–hemes (rHSA–1c, –2c, –5c, –7c and –8c) are almost identical to that of rHSA itself (not shown). This suggests that the secondary structure of the albumin host molecule did not change after incorporation of the hemes. Furthermore, the isoelectric points of these rHSA–hemes were all 4.8, which is the original value of rHSA. The surface net charges of rHSA remained unaltered after heme incorporation.

Dioxygenation of rHSA–heme in aqueous solution

Light irradiation of the CO adduct complex of rHSA–heme (rHSA–1c, –2c, –5c, –6c, –7c and –8c) under an N_2 atmosphere led to CO dissociation and demonstrated new spectral patterns with well-defined α and β bands. For example, the typical absorption spectral changes of rHSA–2c are shown in Fig. 2.

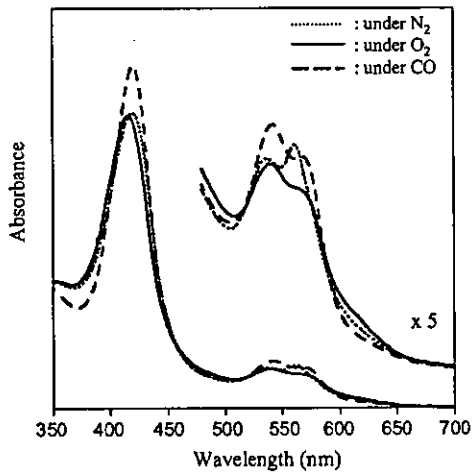

Fig. 2 UV-vis spectra of rHSA–2c in phosphate buffer solution (pH 7.3) at 25 °C.

From the nature of these spectra, we concluded that the obtained Fe(II) complexes are a mixture of Fe(II) 5-coordinated (high-spin) and 6-coordinated (low spin) species. It implies that the sixth coordinate position of the heme might be partially occupied by some amino acid residue of the protein scaffold. Upon exposure of O_2 to the Fe(II) complex of rHSA–1c, the spectrum changed to that of the O_2 adduct species. Although the aqueous micelle solution of 1c with 5% surfactant (cetyltrimethylammonium bromide) forms a CO adduct complex, dioxygenation was not stable enough to measure the spectrum at 25 °C.[7e] In contrast, rHSA–1c, –2c, –5c, and –8c formed O_2 adduct complexes at 25 °C (pH 7.3) except for rHSA–6c and –7c (Table 2). The introduction of a methyl group to the 2-position of the imidazole ring is widely recognized to reduce the O_2 and CO binding affinities.[1] In this case, the strength of the imidazole coordination to the Fe(II) center is too weak to produce a stable O_2 adduct complex.

Table 3 Half-life ($\tau_{1/2}$) and O_2 binding affinity ($P_{1/2}$) of rHSA–hemes in phosphate buffer solution (pH 7.3) at 25 °C

Compounds	$\tau_{1/2}$/min	$P_{1/2}$/Torr
rHSA–1c	20	0.1
rHSA–2c	50	0.1
rHSA–5c	90	0.1
rHSA–8c	50	0.4

The oxidation process of dioxygenated rHSA–heme to the inactive Fe(III) state obeyed first-order kinetics. This indicates that the μ-oxo dimer formation was prevented by the immobilization of heme in the albumin structure. The half-life of the O_2 adduct complexes ($\tau_{1/2}$) and the O_2 binding affinities ($P_{1/2}$) of rHSA–hemes are summarized in Table 3. The histidylglycyl tail coordinated protoheme (5c) in rHSA showed the most stable O_2 adduct complex ($\tau_{1/2}$: 90 min) with respect to the imidazole bound ones. The more hydrophobic ethylpropionate (2c) also contributed to prolong the stability of the O_2 adduct complex relative to the methylpropionate protoheme (1c).

The $P_{1/2}$ values of rHSA–1c, –2c and –5c are 0.1 Torr at 25 °C. On the other hand, rHSA–8c showed a higher $P_{1/2}$ value (low O_2-binding affinity) compared to the others. The acetyl groups at the 3,8-positions of 8c decrease the electron density of the porphyrin macrocycle, therefore $P_{1/2}$ could be significantly reduced. Traylor and co-workers found that the O_2 binding affinity of the chelated heme was sensitive to the electron density at Fe(II) and thus to the substituents at the heme periphery. The O_2 binding constant decreased by 1/6 upon changing the substituent from a vinyl to an acetyl group.[12] Our experimental data of hemes in rHSA are quite consistent with their observations.

Conclusion

A convenient one-pot synthesis of protoporphyrin IX derivatives with a covalently linked proximal base has been described. rHSA successfully incorporates the protoheme derivatives, providing an artificial hemoprotein, which can form an O_2 adduct complex at 25 °C. The rHSA–heme, in which the histidylglycil tail intramolecularly coordinates to the Fe(II) center, showed the most stable O_2 adduct complex with the relatively high O_2 binding affinity of 0.1 Torr.

Experimental

Materials and apparatus

All reagents were used as supplied commercially unless otherwise noted. All solvents were normally purified by distillation before use. DMF was distilled under reduced pressure in N_2. Pyridine was refluxed over and distilled from P_2O_5. The water was deionized using an ADVANTEC GS-200 system. The rHSA (Albrec®, 25 wt%) was obtained from NIPRO Corp. (Osaka).

Thin-layer chromatography was carried out on 0.2 mm precoated plates of silica gel 60 F254 (Merck). Purification was performed by silica gel 60 (Merck) column chromatography. The infrared spectra were measured with a JASCO FT/IR-410 spectrometer. The UV-vis absorption spectra were recorded by a JASCO V-570 spectrophotometer. The ^{1}H-NMR spectra were recorded using a JEOL Lambda 500 spectrometer. Chemical shifts were expressed in parts per million downfield from Me_4Si as the internal standard. The FAB-MS spectra were obtained using a JEOL JMS-SX102A spectrometer.

Synthesis of porphyrin derivatives

O-Methyl-L-histidyl-glycine[13] and 4-(*N*-(2-methylimidazolyl))-butylamine[14] were synthesized according to the reported procedures.

3,18-Divinyl-8-(3-methoxycarbonyl)ethyl-12-(3-(*N*-imidazolyl)propylamido)ethyl-2,7,13,17-tetramethylporphyrin (1a). A pyridine (7 mL) solution of 3-(*N*-imidazolyl)propylamine (35 μL, 0.29 mmol) was added dropwise to protoporphyrin IX (200 mg, 0.36 mmol) and benzotriazol-1-yloxytris-(dimethylamino)phosphonium hexafluorophosphate (411 mg, 0.93 mmol) in pyridine (20 mL) and stirred for 30 min at room temperature. The mixture was reacted for 4 h at 40 °C. After the addition of methanol (10 mL), the solution was stirred for another 12 h at 40 °C. The mixture was then poured into a 10% NaCl solution (1 L, 4 °C) and the suspension was centrifuged for 30 min at 7000*g*. The supernatant was discarded and the precipitate was collected and dried *in vacuo*. The residue was chromatographed on a silica gel column using $CHCl_3/CH_3OH$ = 8/1 (v/v) as the eluent. The main band was collected and dried at room temperature for several hours *in vacuo*, giving compound **1a** as a purple solid (75 mg, 20%). R_f = 0.3 ($CHCl_3/CH_3OH$ = 8/1 (v/v)); IR (NaCl) ν = 1731 (C=O, ester), 1646 (C=O, amide) cm^{-1}; UV-vis ($CHCl_3$) λ_{max} = 408, 506, 542, 575, 630 nm; ^{1}H-NMR ($CDCl_3$) δ: −4.0 (s, 2H, inner), 1.8–2.4 (m, 4H, –(CH_2)$_2$–Im), 2.7 (m, 4H, –CH_2–COO–, NH–CH_2–), 3.2 (t, 2H, –CONH–CH_2–), 3.3–3.7 (m, 18H, por–CH_3, –CH_2–CO–, –$COOCH_3$), 4.2 (d, 4H, por–CH_2–), 5.4 (s, 1H, Im), 6.0–6.3 (m, 4H, =CH_2 (vinyl)), 6.4 (d, 1H, Im), 6.6 (d, 1H, Im), 8.0–8.4 (m, 2H, –CH= (vinyl)), 9.7 (m, 4H, *meso*); MS *m/z*: 681.67.

Fe(III) complex of 1a (1b). Iron(II) chloride tetrahydrate (106 mg, 0.53 mmol) was added to a dry DMF (10 mL) solution of **1a** (36 mg, 53 μmol) and 2,6-lutidine (30 μL, 0.27 mmol) under an N_2 atmosphere. The reaction mixture was stirred at 70 °C for 3 h. After confirming the disappearance of the porphyrin's fluorescence (600–800 nm, ex. 400 nm), the solution was cooled to room temperature and poured into 10% NaCl solution (1 L, 4 °C). The suspension was centrifuged for 30 min at 7000*g* and the supernatant was discarded. The precipitate was dried *in vacuo* and chromatographed on a silica gel column using $CHCl_3/CH_3OH$ = 8/1 (v/v) as the eluent. The main band was collected and dried at room temperature for several hours *in vacuo* to give compound **1b** as a brown solid (27 mg, 68%). R_f = 0.3 ($CHCl_3/CH_3OH$ = 8/1); IR (NaCl) ν = 1728 (C=O, ester), 1646 (C=O, amide) cm^{-1}; UV-vis ($CHCl_3$) λ_{max} = 389, 513, 641 nm; HR-MS *m/z*: calcd for $C_{41}H_{43}O_3N_7Fe$: 737.2777, found: 737.2778 [M$^+$].

3,18-Divinyl-8-(3-ethoxycarbonyl)ethyl-12-(3-(*N*-imidazolyl)-propylamido)ethyl-2,7,13,17-tetramethylporphyrin (2a). The synthetic procedure of compound **2a** was the same as that used for **1a** except for using ethanol instead of methanol. Yield 30%; R_f = 0.4 ($CHCl_3/CH_3OH$ = 10/1); IR (NaCl) ν = 1650 (C=O, amide), 1732 (C=O, ester) cm^{-1}; UV-vis ($CHCl_3$) λ_{max} = 409, 544, 580, 633 nm; ^{1}H-NMR ($CDCl_3$) δ: −4.1 (s, 2H, inner-NH), 0.8–0.9 (t, 3H, –COO–CH_2–CH_3), 1.3–1.5 (t, 2H, –CONH–CH_2–CH_2–), 3.0–3.1 (t, 2H, –CH_2–Im), 3.1–3.3 (m, 4H, –CH_2–COO), 3.5–3.7 (m, 12H, por–CH_3), 3.8–3.9 (m, 2H, –COO–CH_2–CH_3), 4.2–4.4 (d, 4H, por–CH_2–), 6.1 (s, 1H, Im), 6.1–6.4 (q, 5H, =CH_2 (vinyl), Im), 6.6–6.7 (d, 1H, Im), 6.9–7.0 (d, 1H, Im), 8.1–8.3 (m, 2H, –CH= (vinyl)), 9.8–10.2 (m, 4H, *meso*); MS *m/z*: 695.29.

Fe(III) complex of 2a (2b). Iron insertion to **2a** was carried out by the same procedure as in the **1b** preparation. Yield 80%; R_f = 0.3 ($CHCl_3/CH_3OH$ = 8/1); IR (NaCl) ν = 1651 (C=O, amide), 1725 (C=O, ester) cm^{-1}, UV-vis ($CHCl_3$) λ_{max} = 406, 520, 578 nm; HR-MS *m/z*: calcd. for $C_{42}H_{45}O_3N_7Fe$: 751.2933, found: 751.2953 [M$^+$].

3,18-Divinyl-8-(3-carboxy)ethyl-12-(3-(*N*-imidazolyl)propyl-amido)ethyl-2,7,13,17-tetramethylporphyrin (3a). Sodium hydroxide (2 N, 4.5 mL) was added to the methanol (10 mL) solution of **2a** (266 mg, 0.38 mmol) and the mixture was stirred for 12 h at room temperature. It was brought to dryness *in vacuo*. Methanol was added to the residue and the mixture was added dropwise to 10% NaCl solution (pH 2, 4 °C). It was centrifuged for 30 min at 7000*g* and the precipitate was collected and dried *in vacuo*, affording compound **3a** as a brown solid (187 mg, 78%), IR (KBr) ν = 1652 (C=O, amide), 1707 (C=O, –COOH) cm^{-1}; UV-vis (DMSO) λ_{max} = 409, 508, 543, 578, 631 nm; ^{1}H-NMR (d_6-DMSO) δ: −3.5 (s, 2H, inner-NH), 1.6–1.7 (t, 2H, –CONH–CH_2–CH_2–), 2.8–2.9 (t, 2H, –CH_2–Im), 3.1–3.3 (m, 2H, –CONH–CH_2–), 3.5–3.9 (m, 12H, por–CH_3), 4.2–4.4 (d, 4H, por–CH_2–), 6.1 (s, 1H, Im), 6.1–6.4 (q, 5H, =CH_2 (vinyl), Im), 6.6–6.7 (d, 1H, Im), 6.9–7.0 (d, 1H, Im), 8.5–8.6 (m, 2H, –CH= (vinyl)), 10.2–10.4 (m, 4H, *meso*); MS *m/z*: 670.41.

Fe(III) complex of 3a (3b). Iron insertion to **3a** was carried out by the same procedure as in the **1b** preparation. Yield 80%; IR (KBr) ν = 1646 (C=O, amide), 1707 (C=O, –COOH) cm^{-1}; UV-vis (DMSO) λ_{max} = 403, 508, 631 nm; HR-MS *m/z*: calcd. for $C_{40}H_{41}O_3N_7Fe$: 723.2620, found: 724.2668 [M + H$^+$].

3,18-Divinyl-8-(3-methylamido)ethyl-12-(3-(*N*-imidazolyl)-propylamido)ethyl-2,7,13,17-tetramethylporphyrin (4a). Compound **4a** was synthesized according to the same procedure as for **1a** except for using methyl amine instead of methanol. Yield 20%; R_f = 0.5 ($CHCl_3/CH_3OH$ = 3/1); IR (NaCl) ν = 1631 (C=O, amide) cm^{-1}; UV-vis ($CHCl_3$) λ_{max} = 409, 509, 543, 579, 632 nm; ^{1}H-NMR (CD_3OD, $CDCl_3$) δ: −4.0 (s, 2H, inner), 1.8–2.4 (m, 4H, –(CH_2)$_2$–Im), 2.5 (t, 3H, –CONH–CH_3), 2.9 (m, 2H, –CONH–CH_2–), 3.3 (m, 4H, –CH_2–CONH–), 3.4–3.6 (m,12H, por–CH_3), 5.5 (s, 1H, Im), 6.0 (s, 1H, Im), 6.1–6.4 (m, 4H, =CH_2 (vinyl)), 6.8 (m, 1H, Im), 8.1–8.3 (m, 2H, –CH= (vinyl)), 9.7–9.9 (q, 4H, *meso*); MS *m/z*: 680.69.

Fe(III) complex of 4a (4b). Iron insertion to **4a** was carried out by the same procedure as in the **1b** preparation. Yield 67%; R_f = 0.3 ($CHCl_3/CH_3OH$ = 5/1); IR (NaCl) ν = 1646 (C=O, amide) cm^{-1}; UV-vis ($CHCl_3$) λ_{max} = 408, 521, 565 nm; HR-MS *m/z*: calcd. for $C_{41}H_{44}O_3N_7Fe$: 736.2937, found: 736.2938 [M$^+$].

3,18-Divinyl-8-(3-ethoxycarbonyl)ethyl-12-(((3-*N*-glycyl-L-histidinyl)-9-oxymethyl)carbonyl)ethyl-2,7,13,17-tetramethylporphyrin (5a). The synthetic procedure of compound **5a** was same as that used for **1a**. DMF was used instead of pyridine, because it dissolves *O*-methyl-L-histidyl-glycine. Yield 15%; R_f = 0.4 ($CHCl_3/CH_3OH$ = 15/1); IR (NaCl) ν = 1635 (C=O, amide), 1725 (C=O, ester) cm^{-1}; UV-vis ($CHCl_3$) λ_{max} = 405, 505, 541, 577, 627 nm; ^{1}H-NMR ($CDCl_3$) δ: −4.6 (s, 2H, inner-NH), 2.7–2.9 (m, 2H, Im–CH_2–), 3.0–3.5 (m, 18H, por–CH_3, –CH_2–CH_2–CO–NH–, –CH_2–CH_2–COO–CH_2–CH_3), 3.6 (s, 2H, –CONH–CH_2–CONH–), 3.8 (s, 3H,–OCH_3), 4.0–4.3 (d, 4H, por–CH_2–), 4.3–4.5 (m, 1H, α-CH), 6.0–6.4 (m, 4H, =CH_2 (vinyl)), 7.4 (s, 1H, Im–H), 8.0–8.3 (m, 5H, –CH= (vinyl), Im–H), 9.8–10.0 (m, 4H, *meso*-H); MS *m/z*: 782.68.

Fe(III) complex of 5a (5b). Iron insertion to **5a** was carried out by the same procedure as in the **1b** preparation. Yield 75%; R_f = 0.5 ($CHCl_3/CH_3OH$ = 8/1); IR (NaCl) ν = 1660 (C=O, amide), 1734 (C=O, ester) cm^{-1}; UV-vis ($CHCl_3$) λ_{max} = 388, 508, 637 nm; HR-MS *m/z*: calcd. for $C_{44}H_{46}O_6N_8Fe$: 838.2890, found: 839.2929 [M + H$^+$].

3,18-Divinyl-8-(3-ethoxycarbonyl)ethyl-12-(4-(*N*-(2-methyl-imidazolyl))butylamido)ethyl-2,7,13,17-tetramethylporphyrin (6a). Compound **6a** was synthesized by the same procedure as for **1a** except for using 4-(*N*-(2-methylimidazolyl))butylamine instead of 3-imidazolylpropylamine. Yield 20%; R_f: 0.1 ($CHCl_3$/CH_3OH = 8/1); IR (NaCl) ν = 1732 (C=O, ester), 1651 (C=O, amide) cm^{-1}; UV-vis ($CHCl_3$) λ_{max} = 408, 506, 542, 576, 630 nm; ^{1}H-NMR ($CDCl_3$) δ: −4.2 (s, 2H, inner-H), 0.4–0.6 (m, 4H, CONH–CH_2–(CH_2)$_2$–), 1.4–1.5 (d, 3H, Im–CH_3), 2.2–2.4 (m,